AD-A042 560 HUGHES RESEARCH LABS MALIBU CALIF F/G 14/2
ROTATING GRAVITY GRADIOMETER DEVELOPMENT. VOLUME 2. ANALYSIS OF--ETC(U)
APR 77 F19628-76-C-0107
UNCLASSIFIED AFGL-TR-77-0098-2 NL

1 OF 1
ADA042560

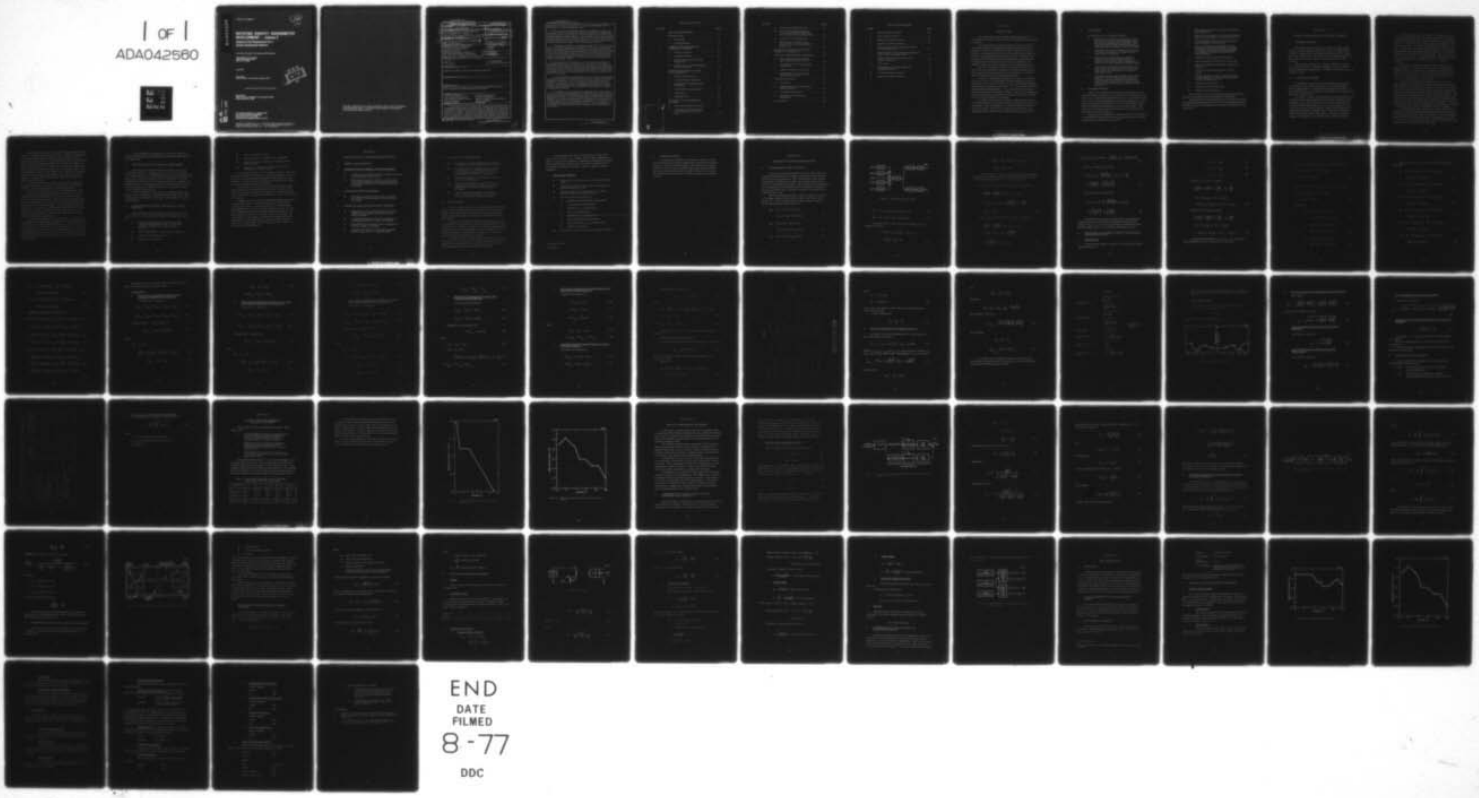

END
DATE FILMED
8-77
DDC

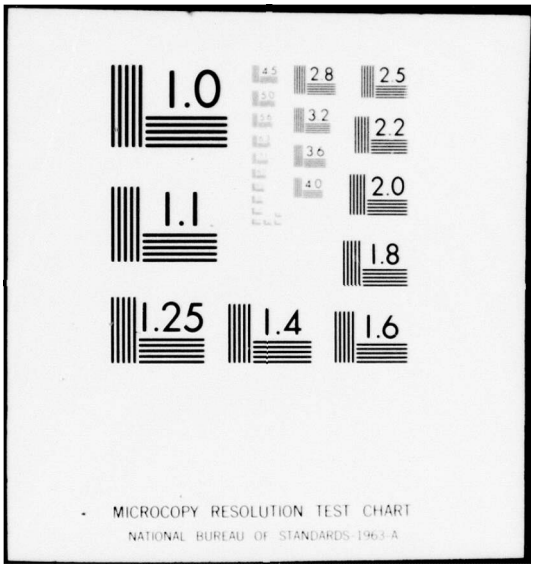
1.0
1.1
1.25
1.4
1.6
1.8
2.0
2.2
2.5
2.8
3.2
3.6
4.0
4.5
5.0
MICROCOPY RESOLUTION TEST CHART
NATIONAL BUREAU OF STANDARDS-1963-A

AFGL-TR-77-0098 (II)

12
NW

ROTATING GRAVITY GRADIOMETER DEVELOPMENT - Volume 2

Analysis of the Requirements for a Gravity Gradiometer Platform

C.B. Ames, R.B. Clark, P.M. LaHue, and R.W. Peterson

Hughes Research Laboratories
3011 Malibu Canyon Road
Malibu, CA 90265

April 1977

Final Report
Period 1 August 1975 through 31 January 1977

Approved for public release; distribution unlimited.

Sponsored by
Defense Advanced Research Projects Agencies (DOD)
ARPA ORDER NO. 2895

AIR FORCE GEOPHYSICS LABORATORY
AIR FORCE SYSTEMS COMMAND
UNITED STATES AIR FORCE
HANSCOM AFB, MASSACHUSETTS 01731

UNCLASSIFIED

SECURITY CLASSIFICATION OF THIS PAGE (When Data Entered)

REPORT DOCUMENTATION PAGE	READ INSTRUCTIONS BEFORE COMPLETING FORM
1. REPORT NUMBER: AFGL-TR-77-0098 (II) -2	2. GOVT ACCESSION NO. / 3. RECIPIENT'S CATALOG NUMBER
4. TITLE (and Subtitle): ROTATING GRAVITY GRADIOMETER DEVELOPMENT • Volume 2. Analysis of the Requirements for a Gravity Gradiometer Platform	5. TYPE OF REPORT & PERIOD COVERED: Final Report 1 Aug 75 - 31 Jan 77
	6. PERFORMING ORG. REPORT NUMBER
7. AUTHOR(s): C. B. Ames, R. B. Clark, P. M. LaHue, and R. W. Peterson	8. CONTRACT OR GRANT NUMBER(s): F19628-76-C-0107
9. PERFORMING ORGANIZATION NAME AND ADDRESS: Hughes Research Laboratories, 3011 Malibu Canyon Road, Malibu, CA 90265	10. PROGRAM ELEMENT, PROJECT, TASK AREA & WORK UNIT NUMBERS: 76000601, 62701E
11. CONTROLLING OFFICE NAME AND ADDRESS: Air Force Geophysics Laboratory, Hanscom AFB, Massachusetts 01731, Monitor/Jack A. Cook, Lt. Col. USAF/LW	12. REPORT DATE: April 1977
	13. NUMBER OF PAGES: 74
14. MONITORING AGENCY NAME & ADDRESS (if different from Controlling Office): 1266 P.	15. SECURITY CLASS. (of this report): UNCLASSIFIED
	15a. DECLASSIFICATION DOWNGRADING SCHEDULE

16. DISTRIBUTION STATEMENT (of this Report)

Approved for public release; distribution unlimited.

17. DISTRIBUTION STATEMENT (of the abstract entered in Block 20, if different from Report)

18. SUPPLEMENTARY NOTES

This research was sponsored by the Defense Advanced Research Projects Agencies (DOD) ARPA Order No. 2895.

19. KEY WORDS (Continue on reverse side if necessary and identify by block number)

Gravity Gradiometer	Airborne Gradiometer
Gravitational Mass Sensor	Vertical Deflection
Gravitational Gradient Sensor	Motion Isolation and Stabilization
Gravity Mapping	Inertial Guidance
Mass Detection	Navigation

20. ABSTRACT (Continue on reverse side if necessary and identify by block number)

The purpose of this contract was to further the development of the Hughes Rotating Gravity Gradiometer (RGG); this effort is a direct continuation of two prior Air Force contracts (F19268-72-C-0222 and F19628-75-C-0201). The stated performance objective for these contracts was the design, construction and demonstration of the Rotating Gravity Gradiometer capable of operating in an airborne environment and producing no more than one (1) Eötvös Unit (EU) of noise, at an

next page

DD FORM 1 JAN 73 1473 EDITION OF 1 NOV 65 IS OBSOLETE

UNCLASSIFIED

SECURITY CLASSIFICATION OF THIS PAGE (When Data Entered)

112600

equivalent ten second integration time, in the determination of the components of a gravity gradient tensor.

The scope of effort ~~in this contract~~ was limited to studies and performance tests and demonstrations in the laboratory environment. Two RGG sensors were involved. The first, RGG-1, was built in 1974 and 1975 under the prior contracts. The second, RGG-2, was designed and built during the course of this contract. The initial scope of work included various tasks to test and modify RGG-1, with the goal of determining configuration changes to be incorporated in RGG-2.

The design for RGG-2 was frozen in April 1976; however, RGG-1 testing continued through November 1976. RGG-2 was assembled and ready for grooming and initial performance evaluations by December 1976. Since this contract was completed on 31 January 1977, the period of RGG-2 performance evaluation was limited to a brief span of a few weeks. However, during that short time, it was conclusively demonstrated that significant progress had been made toward achieving the ultimate performance goals.

Specifically, the performance results obtained with RGG-2 demonstrate that: (1) the design goals have been met for thermal and electronics noise; (2) The sensor output noise goals have nearly been met for the vertical spin axis orientation; (3) Considerable optimism is warranted that the sensor output noise goals can be met for the horizontal spin axis orientation; and (4) Continued development is both necessary and warranted.

A second purpose of this contract was to study the requirements of a platform needed to stabilize up to three RGG sensor in an airborne mapping environment. The results of this study, conducted under subcontract by Incosym, Inc., is reported in Volume II of this Final Report. The study results are encouraging, particularly because an existing DoD platform has been identified as being suitable to support a triad of RGG sensors.

In summary, the availability of a platform and the performance success of RGG-2 permit immediate consideration of a follow-on program which would test and demonstrate all the components of a gravity gradiometer system. It is the recommendation of this report that the Hughes RGG sensor be integrated with a platform at the earliest possible time, and tested in the laboratory environment. It is also the recommendation of this report that the RGG-1 sensor be retrofitted up to the RGG-2 configuration to permit simultaneous development and test efforts.

TABLE OF CONTENTS

SECTION		PAGE
	LIST OF ILLUSTRATIONS	5
1	INTRODUCTION	7
	A. Conclusions	8
	B. Recommendations	8
2	LIAISON WITH PLATFORM AND COMPONENT VENDORS	11
	A. Purpose and Scope	11
	B. Available Hardware	11
	C. Industry Reaction to the VIALS Requirement	14
	D. Modifications to Existing Hardware and Costs Involved	14
3	GROUND RULES FOR PLATFORM DEFINITION STUDY	17
	A. Mission Characteristics	17
	B. Available Support Equipment	17
	C. Method of Data Taking and Data Processing	17
	D. VIALS and RGG Configuration	18
	E. Performance	18
	F. Additional Notes	20
4	REVIEW OF RGG PERFORMANCE FACTORS	21
	A. Mathematical Model of the RGG	21
	B. Evaluation of RGG Sensitivities to Translational Acceleration Inputs	24

SECTION			PAGE
	C.	Narrow Band Random Process	34
	D.	Derivation of Working Equations for Evaluation of RGG Errors Due to Translational Acceleration Inputs . . .	39
	E.	Errors Due to Misalignments	41
	F.	RGG Angular Vibrations Error Measure for Establishing Platform Requirements	43
5		REVIEW OF DATA AND ANALYSIS OF AIRBORNE ENVIRONMENT	45
6		STUDY OF COMPENSATION TECHNIQUES . .	49
	A.	Compensation of the RGG Output for the Rotational Field Effects	49
	B.	Description of the Incoflex Angular Velocimeter	57
	C.	Angular Velocimter Experiment	61
	D.	Compensation of the RGG Output for Anisoelastic Effects	65
7		VIALS SPECIFICATION	67
	A.	Description	67
	B.	VIALS Requirements for Airborne Mapping Mission	67
	C.	Environment—Operating	67
	D.	Functional and Performance Requirement	68
		REFERENCES	74

LIST OF ILLUSTRATIONS

FIGURE		PAGE
1	RGG signal process model	22
2	Power spectral density	39
3	Angular rate power spectrum	47
4	Angular rate power spectrum	48
5	Block diagram of the compensation process for the rotation fields	51
6	Block diagram of the equivalent compensation process for the rotational fields	55
7	Cross section of the two axis incoflex angular velocimeter	58
8	Test set-up	62
9	Compensation of the RGG (SAW) for anisoelastic effects	66
10	Acceleration power spectra	69
11	Angular rate power spectrum	70

SECTION 1

INTRODUCTION

This report defines the Vibration Isolation Alignment and Leveling System (VIALS) requirement for the Rotating Gravity Gradiometer (RGG).

The report defines the RGG performance sensitivities to its environment (angular and translational inputs, heading and tilt etc.) analyzes the expected environment for flight testing, examines the amount of compensation for errors that is desirable and possible, and presents a specification generated from this data. The report also examines the VIALS questions of the availability and applicability of existing hardware and compares them with the feasibility of new hardware design, and makes a tradeoff study of the potential costs.

The first and major question to be resolved was whether the state-of-the-art technology in platforms, vibration isolation systems, and instruments could in fact meet the requirements: we concluded that the requirement is both feasible and practical.

Two areas will require technology that is only just emerging. The first of these is the translational vibration isolation system; the realization of the assumed requirements of a 2-Hz bandwidth isolation is being pursued vigorously in industry. The results obtained thus far indicate good technical progress. The second area is the measurement and compensation of angular vibration. In this case an adaptation of a tuned-rotor gyro to an angular accelerometer showed in preliminary tests that the problem was solvable.

A platform was located that could be modified readily to meet the VIALS requirement, and will satisfy the requirements of form, fit, and function. With the addition of the vibration isolation mount that is being developed, and possibly the angular accelerometers, this modified platform would meet the VIALS performance requirement.

A. CONCLUSIONS

The following are the conclusions reached:

1. It appears to be feasible and practical to mount three of the present-configuration Hughes Rotating Gravity Gradiometers on a platform. Such a platform would be small enough and would perform adequately for laboratory and flight testing.

2. A platform that could be modified easily and that is suitable for laboratory and flight tests does exist, and is in production.

3. Measurement of the rotational vibrations of either a new or modified platform will be required to determine if active compensation is necessary for either laboratory or flight testing.

4. Addition of a low-frequency translational mount to the existing platform might be necessary for flight testing, but would not be necessary for laboratory testing.

5. Laboratory testing could determine the performance of the present RGG design on a practical platform, verify the validity of the RGG mathematical model, and specify the required translational and rotational vibration requirements more accurately.

B. RECOMMENDATIONS

Before a true evaluation of the potential performance of any instrument can be established, it is necessary to test data with the instrument in it's operational configuration and in a "real world" environment. For the Gravity Gradiometer this means mounting it on a platform and finding out how it will react, first in the laboratory under induced environmental conditions, and then in actual flights. Until such tests are performed any design parameters and projections of performance are only estimates.

Because of the availability of suitable hardware, and because of the desirability of obtaining operational performance data, INCOSYM recommends the following steps be taken:

1. Procure (buy or borrow from DoD) an Autonetics Mark II platform.

2. Modify it for laboratory testing, including control gyros and accelerometers, and mount one RGG.

3. Take performance data, monitoring rotational and translational vibration levels.

4. Induce rotational and translational vibration: rotational by inserting a controlled ac voltage to the gimbal torque motors and translational by mounting on a shaker and monitoring the RGG performance.

5. Compare actual to predicted performance.

6. Add a second RGG and observe the cross-talk.

7. Define any software compensation required for flight tests.

8. Define the system mechanization for flight testing.

9. Procure additional hardware required for flight testing (computer, master inertial navigation system, mounting rack etc.).

10. Integrate the full system.

11. Laboratory-test the full system.

12. Flight test the full system.

The above list is extensive and would require approximately two years after procurement of the platform to implement.

The laboratory testing and definition of the flight system could be accomplished during the first year, and the integration, laboratory and flight testing of the complete system could be accomplished in the second year.

SECTION 2

LIAISON WITH PLATFORM AND COMPONENT VENDORS

A. PURPOSE AND SCOPE

The purpose of the liaison was (1) to find out what available hardware could be applied to the VIALS problem, (2) determine the reaction of industry to the feasibility and practicality of the requirement, and (3) obtain data on the modifications to existing hardware or the amount of new design required, and on the respective costs involved.

The following vendors were contacted: Autonetics, Sperry, Litton, Singer-Kearfott, Honeywell, Northrop, Delco, and Actron. We also studied data available from Aeroflex, Carco Electronics, and Contraves-Goertz.

B. AVAILABLE HARDWARE

Investigation revealed one available platform that appears to be attractive for the VIALS requirement. This is the Autonetics Mark II SINS platform. It has the most desirable gimbal order, i.e., the azimuth gimbal is on the outside, which results in the minimum size possible to carry the RGG.

The RGGs could be mounted where the present SINS gyros are mounted with very little modification to the gimbal, and there would be plenty of room left to mount control gyros and accelerometers. The outer thermal shield (which is water cooled) should be removed to give more space around the gimbal. Water cooling should not be required for the VIALS, especially not in a flight test, and replacement of the present shroud would result in a simpler and smaller package. The design of a new shroud would be relatively simple.

The gimbal structure is as small as is practical for a two- or three-RGG package. It is interesting to note that it can be used with either two or three RGGs with no modification to the gimbals, and even if a specific two-RGG configuration were designed, it would not be any smaller. The gimbal is approximately 24 inches in diameter, 20 inches high, and weighs about 220 pounds. With all instruments mounted the whole package should weigh less than 350 pounds. The gimbals are attached to a post through the center, which is convenient for attachment to a mounting structure. The gimbal freedom is at least 40 degrees in pitch and roll, and is 360 degrees in azimuth.

This gimbal configuration puts the center of the RGGs at approximately a 16-inch radius from the center of rotation of the azimuth. However, as the RGGs will have to be calibrated on the system for mass proximities anyway, this does not appear to be a constraint. Any packaging concept will require the centers of the RGGs to be displaced by at least 7 inches.

The gimbal readouts are inductosyns with an accuracy of approximately 10 arcseconds and virtually infinite analog resolution. This would make it possible to slave the RGG platform from a master system in the vehicle provided the master system had an equivalent gimbal order and equivalent gimbal readout accuracy resolution. This would eliminate the requirement for gyros and accelerometers on the RGG platform, but would require a stiff mounting surface between the systems to eliminate any body bending motions, and either a common vibration isolation mount for both systems or a mount that is individual to each system but is "tuned" so that both mounts are identical.

The elimination of the control gyros from the platform would eliminate a source of vibration; the design difficulty of the isolation mount may preclude such an approach, however. The present platform does not have a 2 Hz translational mount, but Autonetics is working on a 2 Hz mount which could be applied for the RGG application. This mount should be available within a few months.

This Autonetics platform utilizes ball bearings between gimbals and has an azimuth slip ring (with 150 rings). These have friction that could cause spurious angular vibrations of the platform. The slip rings could be bypassed by a cable; although this would limit the number of 360° rotations per flight to perhaps 20, it should be acceptable for flight testing. However, as a result of the work done on angular vibration compensation, discussed in Section 6, it would appear that a ball-bearing platform with slip rings could be used. There is no data available on the angular noise on this platform, therefore tests would be required. Refurbishment of the bearings would be advisable if the platform has been in use.

A star tracker has been mounted on one of these Autonetics platforms and has been van tested: the detailed data is not readily available, but in general the system worked satisfactorily.

There is no visible technical reason why this platform could not be modified and flight-tested with RGGs installed, and it is our conclusion that such an approach could be made to work for flight tests. For shipboard applications, the use of such a platform slaved from the SINS appears to be very attractive, as the space would allow both systems to be mounted together. No other platform presently available was as attractive as the Autonetics Mark II SINS for various reasons. In general, the deficiencies of the other platforms were: inferior gimbal arrangement, size either too large or too small, or extensive modification requirements.

If velocity damping from an onboard system were used there are numerous gyros that would be satisfactory as control gyros for the RGG platform. It would probably be best to use a gas-bearing gyro, as they generate lower vibrations than do ball-bearing gyros. The angular vibration of the gimbal with the servo loop closed will be the most important factor in gyro selection, therefore the characteristics of the servo electronics and gimbals will have to be considered carefully when selecting a gyro.

The accelerometer presently used on the Mark II SINS is an example of the available inertial-grade accelerometers that would meet the requirement.

C. INDUSTRY REACTION TO THE VIALS REQUIREMENT

The one area of concern to nearly all vendors was the 2-Hz translational isolation. Autonetics claims to be close to a solution for a payload of this size, although they declined to specify the approach used. Also, Actron has isolated a payload of nearly the exact size postulated for VIALS down to 4 Hz, using a passive (i.e., springs and dampers) system. The major question to be resolved is whether or not an active (penumatic or hydraulic) system will be required instead of a passive spring-damper system.

There is also general uncertainty as to what the angular vibration levels are on platforms, especially at higher frequencies. That problem has been addressed in this report in the section on compensation techniques.

D. MODIFICATIONS TO EXISTING HARDWARE AND COSTS INVOLVED

The modifications to the Autonetics platform needed for it to carry the RGGs have already been outlined. To summarize, these are:

- Modify the mounting slots for the present SINS gyros to accommodate the RGGs. If two RGGs are used, a dummy mass would be used in slot No. 3.
- Add mounting pads for control gyros if required.
- Leave accelerometer slots as is.
- Implement a new shroud.

- Add a 2-Hz isolation mount.
- Design and build a mounting rack for flight test.
- Modify the gimbal control loops if onboard control gyros are used.
- Implement a mechanical and electrical interface if external slave control is used.

If an Autonetics system in a slaved mode is used for the master system then the electrical interface is already established. The cost to modify an available Autonetics platform would be approximately $250,000. To design and build a platform specifically for the requirement would cost approximately $1,000,000.

If the system is slaved the master would probably be a SINS system that would cost nearly $1,000,000. Even if it isn't slaved a very accurate onboard system will be required for initialization and velocity information. A Honeywell GEANS system can be used if slaving is not required.

GEANS systems have been demonstrating flights with guidance accuracy better than 0.1 nautical mile per hour, which would be accurate enough to use as a master reference for 10-hour flights. The GEANS systems are not in volume production, so they are expensive, although they should be somewhat less than SINS system. As spare Autonetics systems are available in the DOD inventory, and as the platform could readily be returned to its original state after modification, it would appear that two of these systems could be borrowed for flight testing, and the only cost incurred would be for modification and refurbishment.

SECTION 3

GROUND RULES FOR PLATFORM DEFINITION STUDY

A. MISSION CHARACTERISTICS

1. Operational Airborne Mapping of the Gravity Gradients

- Duration of one mapping mission is 10 hours max plus any preflight time as necessary.
- Environment typical of C-141 or C-135 aircraft in good weather conditions (benign environment characterized by straight and level flight during taking of the data).

B. AVAILABLE SUPPORT EQUIPMENT

- High-quality inertial reference will be available as a master. The RGG platform will be slaved to the master.

C. METHOD OF DATA TAKING AND DATA PROCESSING

- Flight pattern will be selected such that it will be suitable for bias stability verification by point closure technique.
- In-flight data processing (active compensation) is acceptable provided it is found to be feasible.
- Post-flight data processing is also acceptable provided it is found to be feasible.
- Azimuth VIALS rotation to eliminate turnaround effects may be used if it is found desirable.

D. VIALS AND RGG CONFIGURATION

- Preferable nominal configuration is to consist of a complement of three mutually orthogonal RGGs.
- Second preferable configuration is to consist of a complement of two mutually orthogonal RGGs. (Axis orientation relative to the local vertical and aircraft line of flight is to be defined.)
- Desired RGG platform mechanization is locally level and north pointing.
- The form factor of the existing RGG is to be considered as a breadboard. However, the size and the form of the inner rotor assembly will not change.
- VIALS requirements (platform and isolation system) are to be satisfied in a manner that is most cost effective and schedule effective.

E. PERFORMANCE

Vibration Isolation System parameters should be selected with the objective of reducing spin harmonic errors to acceptable levels without compensation when RGG motion sensitivies are at design goal levels and when external environment is "Defined Operational Environment."

Vibration Isolation System natural frequencies as low as 2 Hz are acceptable for small motions, and non-linear stiffnesses may be employed to limit "High-g" deflections to acceptable magnitudes under transient maneuvers. Active damping may be considered to achieve improved attenuation at spin harmonic frequencies if required but feasibility should be established for hardware.

If (within the prior constraints) any spin harmonic error cannot be reduced to an acceptable level without compensation, then the feasibility of changing the motion sensitivity design goal and/or of compensating the offending error should be determined.

It is assumed that the VIALS cannot limit the rotation field errors and "g^2 errors" to acceptable levels without compensation so that it is necessary to formulate a compensation configuration for these errors such that the residual errors are within acceptable limits in the defined operational environment. (These are <u>not</u> spin harmonic dependent).

1. <u>Error Budget Guidelines</u>

- Total system tensor element error standard deviation ≤1 EU
- RGG self noise tensor element error contributions to standard deviation ≥0.7 EU
- Root sum square of all remaining errors must not exceed 0.7 EU for each tensor element
- The error forms due to VIALS are
  a. Rotation field residual after compensation
  b. g^2 residual after compensation
  c. Diff MU (K_1, K_2) spin harmonic
  d. Axial (K_3) spin harmonic
  e. Dyn MU (K_4, K_5) spin harmonic
  f. Sum-mode MM (K_6) spin harmonic
  g. Skew misalign (K_{11}, K_{12}) spin harmonic
  h. Platform orientation.
- If each error in "D" is 0.25 EU,* the RSS is 0.71 EU.

*One sigma.

F. ADDITIONAL NOTES

It is the primary objective of this effort to provide a VIALS specification that will meet the requirements of the airborne mapping mission. However, the requirements of the longer-time-constant submarine missions and low-altitude flight (more bumpy) oil exploration survey missions should also be listed, and prior to any major decision relative to the airborne VIALS these requirements should be reviewed.

SECTION 4

REVIEW OF RGG PERFORMANCE FACTORS

A. MATHEMATICAL MODEL OF THE RGG

In order to specify the characteristics of the VIALS system we must know the vibrational environment, and also know the sensitivity of the RGG to that environment. The characteristics of the expected environment are addressed in another section of this report; in this section we establish the RGG model. This mathematical model permits us to evaluate the errors resulting from the vibrational environment and thus specify the level of isolation necessary to keep these errors within allowable limits.

The RGG mathematical model is based on equations presented in the Hughes report entitled Rotating Gravity Gradiometer, dated March 1976. The RGG signal process model is shown in Figure 1, and the input functions to this model are:

$$A_{(t)} = A_{1c} \cos \omega_s t + A_{1S} \sin \omega_s t + A_{3c} \cos 3\omega_s t + A_{3s} \sin 3\omega_s t \quad (1)$$

$$B_{(t)} = B_{1c} \cos \omega_s t + B_{1s} \sin \omega_s t + B_{3c} \cos 3\omega_s t + B_{3s} \sin 3\omega_s t \quad (2)$$

$$C_{(t)} = C_{2c} \cos 2\omega_s t + C_{2s} \sin 2\omega_s t \quad (3)$$

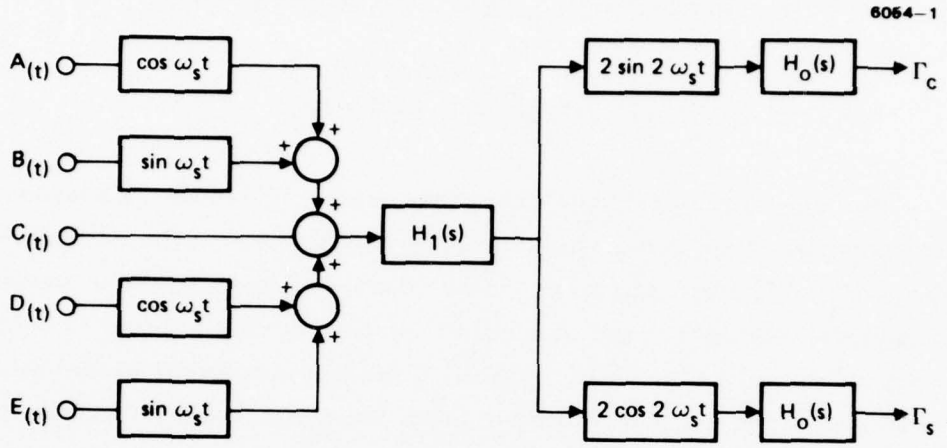

Figure 1. RGG signal process model.

$$D_{(t)} = D_0 + D_{4c} \cos 4\omega_s t + D_{4s} \sin 4\omega_s t \tag{4}$$

$$E_{(t)} = E_0 + E_{4c} \cos 4\omega_s t + E_{4s} \sin 4\omega_s t \tag{5}$$

The output signals of the RGG process model are given by Equations (6) and (7)

$$\Gamma_c = \frac{1}{2}(A_{1s} + B_{1c}) + \frac{1}{2}(A_{3s} - B_{3c}) + C_{2s}$$

$$+ \frac{1}{2}(D_{4s} - E_{4c}) + E_0 \tag{6}$$

$$\Gamma_s = \frac{1}{2}(A_{1c} - B_{1s}) + \frac{1}{2}(A_{3c} + B_{3s}) + C_{2c}$$

$$+ \frac{1}{2}(D_{4c} + E_{4s}) + D_0 \qquad (7)$$

The five input time functions contain gravity gradient signals, rotational field gradient signals, and motion sensitive error signals, and are stated by equations (8), (9), (11), (12), and (13)

$$A_{1c} \cos \omega_s t + A_{1s} \sin \omega_s t + A_{3c} \cos 3\omega_s t + A_{3s} \sin 3\omega_s t$$

$$= K_1\left(\frac{a_x}{g}\right) + K_2\left(\frac{a_y}{g}\right) + K_4(\omega_x - \omega_y\ \omega_z + \Gamma_{yz})$$

$$+ K_5(\dot{\omega}_y + \omega_x\omega_z - \Gamma_{xz}) + K_9\left(\frac{a_y a_z}{g^2}\right) - K_{10}\ \frac{a_x a_z}{g^2}$$

$$+ K_{11}\omega_y - K_{12}\omega_x \qquad (8)$$

$$B_{1c} \cos \omega_s t + B_{1s} \sin \omega_s t + B_{3c} \cos 3\omega_s t + B_{3s} \sin 3\omega_s t$$

$$= K_1\left(\frac{a_y}{g}\right. - K_2\left(\frac{a_x}{g}\right) + K_4(\dot{\omega} + \omega_x\omega_z - \Gamma_{xz})$$

$$- K_5(\dot{\omega}_x - \omega_y\omega_z + \Gamma_{yz}) - K_9\left(\frac{a_x a_z}{g^2}\right)$$

$$- K_{10}\left(\frac{a_y a_z}{g^2}\right) - K_{11}\omega_x - K_{12}\omega_y \qquad (9)$$

$$C_{2c} \cos 2\omega_s t + C_{2s} \sin 2\omega_s t = K_3 \left(\frac{a_z}{g}\right) + K_6 \dot{\omega}_z + \text{Thermal noise} \tag{10}$$

$$D_0 + D_{4c} \cos 4\omega_s t + D_{4s} \sin 4\omega_s t$$

$$= 2\Gamma_{xy} - 2\omega_x \omega_y - \left[\frac{\Delta\Phi_{ij}}{\eta c}\right]\left[\Gamma_{yy} - \Gamma_{xx} + \omega_x^2 - \omega_y^2\right]$$

$$+ K_7 \left(\frac{2a_x a_y}{g^2}\right) + K_8 \left[\frac{a_y^2 - a_x^2}{g^2}\right] \tag{11}$$

$$E_0 + E_{4c} \cos 4\omega_s t + E_{4s} \sin 4\omega_s t$$

$$= \Gamma_{yy} - \Gamma_{xx} + \omega_x^2 - \omega_y^2 + \left[\frac{\Delta\Phi_{ij}}{\eta c}\right]\left[2\Gamma_{xy} - 2\omega_x \omega_y\right]$$

$$+ K_7 \left(\frac{a_y^2 - a_x^2}{g^2}\right) - K_8 \left(\frac{2a_x a_y}{g^2}\right) \tag{12}$$

Once the form of the input functions of the gravity gradients, rotational fields and accelerations is established, then the input coefficients A_{1c}, A_{1s}, etc. are evaluated and are substituted to obtain the RGG outputs Γ_c and Γ_s as indicated by Equations (6) and (7).

B. EVALUATION OF RGG SENSITIVITIES TO TRANSLATIONAL ACCELERATION INPUTS

1. Resolved Form

Assume all other inputs are equal to zero and the acceleration inputs have the form:

$$a_x = g(\eta_x - C_{xg}) \tag{13}$$

$$a_y = g(\eta_y - C_{yg}) \tag{14}$$

$$a_z = g(\eta_z - C_{zg}) \tag{15}$$

Using (13), (14), and (15) evaluate

$$K_1\left(\frac{a_x}{g}\right) + K_2\left(\frac{a_y}{g}\right) + K_9\frac{a_y a_z}{g^2} - K_{10}\frac{a_x a_z}{g^2}$$

$$= (K_1 + K_{10} C_{zg})\eta_x + (K_z - K_9 C_{zg})\eta_y$$

$$+ (K_{10} C_{xg} - K_9 C_{yg})\eta_z + (K_9\eta_y - K_{10}\eta_x)\eta_z \tag{16}$$

Using (13), (14), and (15) evaluate

$$K_1\left(\frac{a_y}{g}\right) - K_2\left(\frac{a_x}{g}\right) - K_9\frac{a_x a_z}{g^2} - K_{10}\frac{a_y a_z}{g^2}$$

$$= (K_1 + K_{10} C_{zg})\eta_y - (K_2 - K_9 C_{zg})\eta_x$$

$$+ (K_{10} C_{yg} + K_9 C_{xg})\eta_z - (K_9\eta_x + K_{10}\eta_y)\eta_z \tag{17}$$

Assuming that the products $\eta_x\eta_z$ and $\eta_y\eta_z$ can be neglected, then substituting (16) and (17) into (8) and (9) we obtain

$$(A_{1c} \cos \omega_s t + A_{1s} \sin \omega_s t) + (A_{3c} \cos 3\omega_s t + A_{3s} \sin 3\omega_s t)$$

$$= (K_1 + K_{10} C_{zg})\eta_x + (K_2 - K_9 C_{zg})\eta_y$$

$$+ (K_{10} C_{xg} - K_9 C_{yg})\eta_z \tag{18}$$

$$(B_{1c} \cos \omega_s t + B_{1s} \sin \omega_s t) + (B_{3c} \cos 3\omega_s t + B_{3s} \sin 3\omega_s t)$$

$$= (K_1 + K_{10} C_{zg})\eta_y - (K_2 - K_9 C_{zg})\eta_x$$

$$+ (K_{10} C_{yg} + K_9 C_{xg})\eta_z \tag{19}$$

Assume that

$$\eta_x = \eta_{x1c} \cos \omega_s t + \eta_{x1s} \sin \omega_s t$$

$$+ \eta_{x3c} \cos 3\omega_s t + \eta_{x3s} \sin 3\omega_s t \tag{20}$$

$$\eta_y = \eta_{y1c} \cos \omega_s t + \eta_{y1s} \sin \omega_s t$$

$$\eta_{y3c} \cos 3\omega_s t + \eta_{y3s} \sin 3\omega_s t \tag{21}$$

$$\eta_z = \eta_{z1c} \cos \omega_s t + \eta_{z1s} \sin \omega_s t$$

$$\eta_{z3c} \cos 3\omega_s t + \eta_{z3s} \sin 3\omega_s t \tag{22}$$

Substitute (20), (21) and (22) into (18) and (19) and compare coefficients

$$A_{1c} = (K_1 + K_{10} C_{zg})\eta_{x1c} + (K_2 - K_9 C_{zg})\eta_{y1c} + (K_{10} C_{xg} - K_9 C_{yg})\eta_{z1c} \quad (23)$$

$$A_{1s} = (K_1 + K_{10} C_{zg})\eta_{x1s} + (K_2 - K_9 C_{zg})\eta_{y1s} + (K_{10} C_{xg} - K_9 C_{yg})\eta_{z1s} \quad (24)$$

$$A_{3c} = (K_1 + K_{10} C_{zg})\eta_{x3c} + (K_2 - K_9 C_{zg})\eta_{y3c} + (K_{10} C_{xg} - K_9 C_{yg})\eta_{z3c} \quad (25)$$

$$A_{3s} = (K_1 + K_{10} C_{zg})\eta_{x3s} + (K_2 - K_9 C_{zg})\eta_{y3s} + (K_{10} C_{xg} - K_9 C_{yg})\eta_{z3s} \quad (26)$$

$$B_{1c} = (K_1 + K_{10} C_{zg})\eta_{y1c} - (K_2 - K_9 C_{zg})\eta_{x1c} + (K_{10} C_{yg} + K_9 C_{xg})\eta_{z1c} \quad (27)$$

$$B_{1s} = (K_1 + K_{10} C_{zg})\eta_{y1s} - (K_2 - K_9 C_{zg})\eta_{x1s} + (K_{10} C_{yg} + K_9 C_{xg})\eta_{z1s} \quad (28)$$

$$B_{3c} = (K_1 + K_{10} C_{zg})\eta_{y3c} - (K_2 - K_9 C_{zg})\eta_{x3c}$$

$$+ (K_{10} C_{yg} + K_9 C_{xg})\eta_{z3c} \tag{29}$$

$$B_{3s} = (K_1 + K_{10} C_{zg})\eta_{y3s} - (K_2 - K_9 C_{zg})\eta_{x3s}$$

$$+ (K_{10} C_{yg} + K_9 C_{xg})\eta_{z3s} \tag{30}$$

Substitute (23) through (30) into (6) and (7)

$$\Gamma_c = \frac{1}{2}(K_1 + K_{10} C_{zg})(\eta_{x1s} + \eta_{y1c}) + \frac{1}{2}(K_2 - K_9 C_{zg})(\eta_{y1s} - \eta_{x1c})$$

$$+ \frac{1}{2}(K_{10} C_{xg} - K_9 C_{yg})\eta_{z1s} + \frac{1}{2}(K_{10} C_{yg} + K_9 C_{xg})\eta_{z1c}$$

$$+ \frac{1}{2}(K_1 + K_{10} C_{zg})(\eta_{x3s} - \eta_{y3c}) + \frac{1}{2}(K_2 - K_9 C_{zg})(\eta_{y3s} + \eta_{x3c})$$

$$+ \frac{1}{2}(K_{10} C_{xg} - K_9 C_{yg})\eta_{z3s} - (K_{10} C_{yg} + K_9 C_{xg})\eta_{z3c} \tag{31}$$

$$\Gamma_s = \frac{1}{2}(K_1 + K_{10} C_{zg})(\eta_{x1c} - \eta_{y1s}) + \frac{1}{2}(K_2 - K_9 C_{zg})(\eta_{y1c} + \eta_{x1s})$$

$$+ \frac{1}{2}(K_{10} C_{xg} - K_9 C_{yg})\eta_{z1c} - (K_{10} C_{yg} + K_9 C_{xg})\eta_{z1s}$$

$$+ \frac{1}{2}(K_1 + K_{10} C_{zg})(\eta_{x3c} + \eta_{y3s}) + \frac{1}{2}(K_2 - K_9 C_{zg})(\eta_{y3c} - \eta_{x3s})$$

$$+ \frac{1}{2}(K_{10} C_{xg} - K_9 C_{yg})\eta_{z3c} - \frac{1}{2}(K_{10} C_{yg} + K_9 C_{xg})\eta_{z3s}$$

(32)

Equations (31) and (32) state the RGG sensitivities to translational acceleration inputs of sinusoidal nature.

2. Complex Form

a. Errors Due to Translational Vibration at Spin Frequency Perpendicular to the Spin Axis

From Eq. (28) of reference 1.

$$\Delta\Gamma_c\Big|_{\eta_1} = P_1\eta_{x1s} - P_2\eta_{x1c} + P_1\eta_{y1c} + P_2\eta_{y1s} \tag{33}$$

$$\Delta\Gamma_s\Big|_{\eta_1} = P_2\eta_{x1s} + P_1\eta_{x1c} + P_2\eta_{y1c} - P_1\eta_{y1s} \tag{34}$$

Multiply (34) by $j = \sqrt{-1}$ and add to (33)

$$\Delta\Gamma_{cs}\Big|_{\eta_1} = (\bar{\eta}_{y1cs} + j\bar{\eta}_{x1cs})P_{12} \tag{35}$$

where

$$P_{12} = P_1 + jP_2$$

$$= \frac{1}{2}\left[K_1 + K_{10}C_{zg}\right] + j\,\frac{1}{2}\left[K_2 - K_9 C_{zg}\right] \tag{36}$$

$$\bar{\eta}_{x1cs} = \eta_{x1c} - j\eta_{x1s} \tag{37}$$

$$\overline{\eta}_{y1cs} = \eta_{y1c} - j\eta_{y1s} \tag{38}$$

$$\Delta\Gamma_{cs}\Big|_{\eta_1} = \Delta\Gamma_c\Big|_{\eta_1} + j\,\Delta\Gamma_s\Big|_{\eta_1}$$

b. Errors Due to Translational Vibration at Three Times Spin Frequency Perpendicular to the Spin Axis

From Eq. (29) of Reference 1

$$\Delta\Gamma_c\Big|_{\eta_3} = P_1\eta_{x3s} + P_2\eta_{x3c} - P_1\eta_{y3c} + P_2\eta_{y3s} \tag{39}$$

$$\Delta\Gamma_s\Big|_{\eta_3} = -P_2\eta_{x3s} + P_1\eta_{x3c} + P_2\eta_{y3c} + P_1\eta_{y3s} \tag{40}$$

Multiply (40) by j and add to (39)

$$\Delta\Gamma_{cs}\Big|_{\eta_3} = (-\overline{\eta}_{y3cs} + j\eta_{x3cs})\,\overline{P}_{12} \tag{41}$$

where

$$\overline{P}_{12} = P_1 - jP_2$$

$$= \frac{1}{2}\left[K_1 + K_{10}\,C_{zg}\right] - j\,\frac{1}{2}\left[K_2 - K_9\,C_{zg}\right] \tag{42}$$

$$\overline{\eta}_{y3cs} = \eta_{y3c} - j\eta_{y3s} \tag{43}$$

$$\bar{\eta}_{x3cs} = \eta_{x3c} - j\eta_{x3s} \tag{44}$$

$$\Delta\Gamma_{cs}\Big|_{\eta_3} = \Delta\Gamma_c\Big|_{\eta_3} + j\,\Delta\Gamma_s\Big|_{\eta_3}$$

c. Errors Due to Translational Vibration at Four Times Spin Frequency Perpendicular to the Spin Axis

From Eq. (33) of Reference 1

$$-\Delta\Gamma_c\Big|_{\eta_4} = P_7\eta_{x4c} + P_8\eta_{y4c} + P_7\eta_{y4s} - P_8\eta_{x4s} \tag{45}$$

$$-\Delta\Gamma_s\Big|_{\eta_4} = -P_8\eta_{x4c} + P_7\eta_{y4c} - P_8\eta_{y4s} - P_7\eta_{x4s} \tag{46}$$

Multiply (46) by j and add to (45)

$$\Delta\Gamma_{cs}\Big|_{\eta_4} = -(\bar{\eta}_{x4cs} + j\bar{\eta}_{y4cs})\,\bar{P}_{78} \tag{47}$$

where

$$\bar{P}_{78} = P_7 - jP_8$$

$$= (K_7 C_{xg} + K_8 C_{yg}) - j(K_8 C_{xg} - K_7 C_{yg}) \tag{48}$$

$$\bar{\eta}_{x4cs} = \eta_{x4c} - j\eta_{x4s} \tag{49}$$

$$\bar{\eta}_{y4cs} = \eta_{y4c} - j\eta_{y4s} \tag{50}$$

$$\Delta\Gamma_{cs}\Big|_{\eta_4} = \Delta\Gamma_c\Big|_{\eta_4} + j\Gamma_s\Big|_{\eta_4} \tag{51}$$

d. Errors Due to Translational Vibration at Spin Frequency Along the Spin Axis

From Eq. (34) of Reference 1

$$\Delta\Gamma_c\Big|_{z1} = P_{10}\eta_{z1s} + P_9\eta_{z1c} \tag{52}$$

$$\Delta\Gamma_s\Big|_{z1} = -P_9\eta_{z1s} + P_{10}\eta_{z1c} \tag{53}$$

Multiply (53) by j and add to (52)

$$\Delta\Gamma_{cs}\Big|_{z1} = \eta_{z1cs}P_{910} \tag{54}$$

where

$$\eta_{z1cs} = \eta_{z1c} + j\eta_{z1s} \tag{55}$$

$$P_{910} = P_9 + jP_{10}$$

$$= \frac{1}{2}\left[K_9 C_{xg} + K_{10} C_{yg}\right] + j\frac{1}{2}\left[K_{10} C_{xg} - K_9 C_{yg}\right] \tag{56}$$

$$\Delta\Gamma_{cs}\Big|_{z1} = \Delta\Gamma_c\Big|_{z1} + j\Delta\Gamma_s\Big|_{z1} \tag{57}$$

e. Errors Due to Translational Vibration Along the Spin Axis at Twice the Spin Frequency

From Eq. (32) of Reference 1

$$\Delta\Gamma_c\Big|_{z2} = K_3\ z2s \tag{58}$$

$$\Delta\Gamma_s\Big|_{z2} = K_3\ z2c \tag{59}$$

$$\Delta\Gamma_{cs}\Big|_{z2} = j\,\bar{\eta}_{z2cs}\,K_3 \tag{60}$$

where

$$\bar{\eta}_{z2cs} = \eta_{z2c} - j\eta_{z2s} \tag{61}$$

$$\Delta\Gamma_{cs}\Big|_{z2} = \Delta\Gamma_c\Big|_{z2} + j\,\Delta\Gamma_s\Big|_{z2} \tag{62}$$

f. Translational Vibration Along the Spin Axis at Three Times Spin Frequency

From Eq. (34) of Reference 1

$$\Delta\Gamma_c\Big|_{z3} = P_{10}\eta_{z3s} - P_9\eta_{z3c} \tag{63}$$

$$\Delta\Gamma_s\Big|_{z3} = P_9\eta_{z3s} + P_{10}\eta_{z3c} \tag{64}$$

Multiply (64) by j and add to (63)

$$\Delta\Gamma_{cs}{}_{z3} = - \bar{\eta}_{z3cs} P_{910} \tag{65}$$

where

$$\bar{P}_{910} = \frac{1}{2}\left[K_9 C_{xg} + K_{10} C_{yg}\right] - j\frac{1}{2}\left[K_{10} C_{xg} - K_9 C_{yg}\right]$$

$$\bar{\eta}_{z3cs} = \eta_{z3c} - j\eta_{z3c} \tag{66}$$

$$\Delta\Gamma_{cs}\Big|_{z3} = \Delta\Gamma_c\Big|_{z3} + j\Delta\Gamma_s\Big|_{z3} \tag{67}$$

Equations (35), (42), (47), (54), (60) and (65) are presented in Table 1.

C. NARROW BAND RANDOM PROCESS

Let the narrow band random process be described by a function

$$y_{(t)} = V_{(t)} \cos(\omega_0 t + \phi_{(t)}) \tag{68}$$

where $V_{(t)}$ and $\phi_{(t)}$ are random variables and the frequency ω_0 is nominally constant.

Expand (68)

$$y_{(t)} = \left[V_{(t)} \cos \phi_{(t)}\right] \cos \omega_0 t - \left[V_{(t)} \sin \phi_{(t)}\right] \sin \omega_0 t$$

$$= y_c \cos \omega_0 t - y_s \sin \omega_0 t \tag{69}$$

Table 1

FORM OF INPUT			
$\eta_{x1}(t) = \eta_{x1c}\cos\omega_s t + \eta_{x1s}\sin\omega_s t$ $\eta_{y1}(t) = \eta_{y1c}\cos\omega_s t + \eta_{y1s}\sin\omega_s t$	$\eta_{x1s} + j\eta_{x1c} + \eta_{y1c} - j\eta_{y1s}$ $\eta_{x1s} + j\eta_{x1c} + \eta_{y1c} - j\eta_{y1s}$	Differential Arm Mass Unb. $\frac{1}{2}(K_1 + jK_2)$ Cross Anisoelastic $\frac{1}{2}(K_{10} - jK_9)C_{zg}$	$\Delta\Gamma_c\big\|_{\eta_1} + j\Delta\Gamma_s\big\|_{\eta_1}$
$\eta_{x3}(t) = \eta_{x3c}\cos 3\omega_s t + \eta_{x3s}\sin 3\omega_s t$ $\eta_{y3}(t) = \eta_{y3c}\cos 3\omega_s t + \eta_{y3s}\sin 3\omega_s t$	$\eta_{x3s} + j\eta_{x3c} - \eta_{y3c} - j\eta_{y3s}$ $\eta_{x3s} + j\eta_{x3c} - \eta_{y3c} - j\eta_{3s}$	Differential Arm Mass Unb. $\frac{1}{2}(K_1 - jK_2)$ Cross Anisoelastic $\frac{1}{2}(K_{10} - jK_9)C_{zg}$	$\Delta\Gamma_c\big\|_{\eta_3} - j\Delta\Gamma_s\big\|_{\eta_3}$
$\eta_{x4}(t) = \eta_{x4c}\cos 4\omega_s t + \eta_{x1s}\sin 4\omega_s t$ $\eta_{y4}(t) = \eta_{y4c}\cos 4\omega_s t + \eta_{y1s}\sin 4\omega_s t$	$-\eta_{x4c} + j\eta_{x4s} - \eta_{y4s} - j\eta_{y4c}$	Prime Anisoelastic $(K_7 - jK_8)C_{xg} - (K_8 + jK_7)C_{yg}$	$\Delta\Gamma_c\big\|_{\eta_4} + j\Delta\Gamma_s\big\|_{\eta_4}$
$\eta_{z1}(t) = \eta_{z1c}\cos\omega_s t + \eta_{z1s}\sin\omega_s t$	$\eta_{z1c} + j\eta_{z1s}$	Cross Anisoelastic $\frac{1}{2}(K_9 + jK_{10})C_{xg} + \frac{1}{2}(K_{10} - jK_9)C_{yg}$	
$\eta_{z2}(t) = \eta_{z2c}\cos 2\omega_s t + \eta_{z2s}\sin 2\omega_s t$	$\eta_{z2c} - j\eta_{z2s}$	Axial Vibr. Torsional Sensitivity jK_3	$\Delta\Gamma_c\big\|_{z2} + j\Delta\Gamma_s\big\|_{z2}$
$\eta_{z3}(t) = \eta_{z3c}\cos 3\omega_s t + \eta_{z3s}\sin 3\omega_s t$	$-\eta_{z3c} + j\eta_{z3s}$	Cross Anisoelastic $\frac{1}{2}(K_9 - jK_{10})C_{xg} + \frac{1}{2}(K_{10} + jK_9)C_{yg}$	$\Delta\Gamma_c\big\|_{z3} + j\Delta\Gamma_s\big\|_{z3}$

ERROR GRADIENT DUE TO TRANSLATIONAL VIBRATIONS

T2149

where

$$y_c = V_{(t)} \cos \phi_{(t)}$$

$$y_s = V_{(t)} \sin \phi_{(t)} \tag{70}$$

and y_c and y_s are random variables that can be characterized by variances $\sigma^2_{y_c}$ and $\sigma^2_{y_s}$.

It will be assumed that

$$\sigma^2_{y_c} = \sigma^2_{y_s} = \sigma^2_y \tag{71}$$

1. Narrow Band Random Process Applied to the RGG

Consider error due to the differential arm mass unbalance in the cosine channel from Table 1

$$\Delta\Gamma_c \Big|_{\eta_1} = (\eta_{x1s} + \eta_{y1c}) \frac{1}{2} K_1 - (\eta_{x1c} - \eta_{y1s}) \frac{1}{2} K_2 . \tag{72}$$

Assume η_{x1s}, η_{y1c}, η_{x1c} and η_{y1s} are characterized by variances σ^2_{x1s}, σ^2_{y1s}, σ^2_{x1c} and σ^2_{y1s} respectively. Thus Equation (72) can be written

$$\sigma_{\Delta\Gamma_c}\Big|_{\eta_1} = \left(\sigma^2_{x1s} + \sigma^2_{y1c}\right)\left(\frac{K_1}{2}\right)^2 + \left(\sigma^2_{x1c} + \sigma^2_{y1z}\right)\left(\frac{K_2}{2}\right)^2 \tag{73}$$

Assuming that

$$\sigma^2_{x1s} = \sigma^2_{x1c} \triangleq \frac{1}{2} \sigma^2_{x1}$$

and

$$\sigma^2_{y1s} = \sigma^2_{y1c} \triangleq \frac{1}{2}\,\sigma^2_{y1}$$

Therefore

$$\sigma^2_{x1s} + \sigma^2_{y1c} = \sigma^2_{x1c} + \sigma^2_{y1s} = \frac{\sigma^2_{x1} + \sigma^2_{y1}}{2}$$

Thus Equation 73 becomes

$$\sigma_{\Delta\Gamma}\Big|_{\eta_1} = \frac{\sigma^2_{x1} + \sigma^2_{y1}}{2}\left[\left(\frac{K_1}{2}\right)^2 + \left(\frac{K_2}{2}\right)^2\right] \tag{74}$$

also assuming

$$\sigma^2_{x1} = \sigma^2_{y1} \triangleq \sigma^2_{1}$$

$$\sigma^2_{\Delta\Gamma_c}\Big|_{\eta_1} = \frac{1}{4}\,(K_1^2 + K_2^2)\;\sigma^2_{\eta_1} \tag{75}$$

In a similar way we evaluate contributions of the other RGG sensitivities and obtain the RGG variance error model for translational spin harmonic vibrations shown in Table 2.

Table 2

		Differential Arm Mass Unb.
Variance of vibrations at ω_s along X and Y	$\sigma^2_{\eta_1}$	$\left(\frac{K_1}{2}\right)^2 + \left(\frac{K_2}{2}\right)^2$
		Cross Anisoelastic
	$\sigma^2_{\eta_1}$	$C^2_{zg}\left[\left(\frac{K_9}{2}\right)^2 + \left(\frac{K_{10}}{2}\right)^2\right]$
		Differential Arm Mass Unb.
	$\sigma^2_{\eta_3}$	$\left(\frac{K_1}{2}\right)^2 + \left(\frac{K_2}{2}\right)^2$
Variance of vibrations at $3\omega_s$ along X and Y		Cross Anisoelastic
	$\sigma^2_{\eta_3}$	$C^2_{zg}\left[\left(\frac{K_9}{2}\right)^2 + \left(\frac{K_{10}}{2}\right)^2\right]$
		Prime Anisoelastic
Variance of vibrations at $4\omega_s$ along X and Y	$\sigma^2_{\eta_4}$	$(C^2_{xg} + C^2_{yg})\left[K^2_7 + K^2_8\right]$
		Cross Anisoelastic
Variance of vibrations at ω_s along Z	σ^2_{z1}	$\frac{1}{2}(C^2_{xg} + C^2_{yg})\left[\left(\frac{K_9}{2}\right)^2 + \left(\frac{K_{10}}{2}\right)^2\right]$
		Axial Vibr. Torsional Sens.
Variance of vibrations at $2\omega_s$ along Z	σ^2_{z2}	$\left(\frac{K_3}{2}\right)^2$
		Cross Anisoelastic
Variance of vibrations at $3\omega_s$ Along Z	σ^2_{z3}	$\frac{1}{2}(C^2_{xg} + C^2_{yg})\left[\left(\frac{K_9}{2}\right)^2 + \left(\frac{K_{10}}{2}\right)^2\right]$

TOTAL VARIANCE PER CHANNEL DUE TO TRANSLATIONAL VIBRATIONS

T2150

D. DERIVATION OF WORKING EQUATIONS FOR EVALUATION OF RGG ERRORS DUE TO TRANSLATIONAL ACCELERATION INPUTS

1. Power Spectral Density

Assume power spectral density to be as shown in Figure 2. The variance for the nth harmonic is

$$\sigma_{\eta}^{2} = 2\Delta fN \tag{75}$$

where $2\Delta f$ for the RGG is equal to 0.1 Hz.

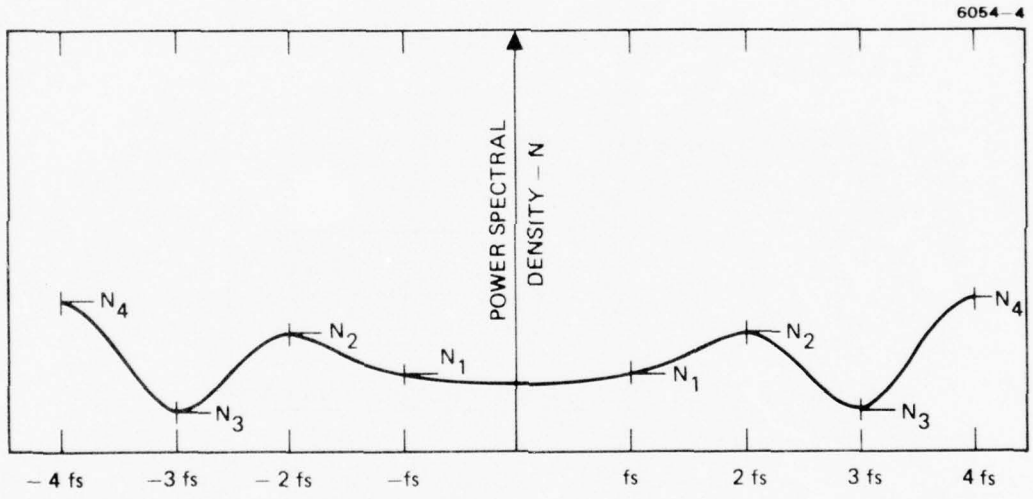

Figure 2. Power spectral density.

2. Error Contribution by the Differential Arm Mass Unbalance

From Table 2

$$\Delta\sigma_{\Delta\Gamma} = \sigma^2_{\eta_1}\left[\left(\frac{K_1}{2}\right)^2 + \left(\frac{K_2}{2}\right)^2\right] + \sigma^2_{\eta_3}\left[\left(\frac{K_1}{2}\right)^2 + \left(\frac{K_2}{2}\right)^2\right] \tag{76}$$

Combining (75) with (76) we obtain

$$\sigma_{\Delta\Gamma} = \sqrt{2\Delta f(N_1 + N_3)\left[\left(\frac{K_1}{2}\right)^2 + \left(\frac{K_2}{2}\right)^2\right]} \tag{77}$$

3. Error Contribution by the Axial Vibration Torsional Sensitivity

From Table 2 and Eq. (75)

$$\sigma_{\Delta\Gamma} = \sqrt{2\Delta f\, N_2\left(\frac{K_3}{2}\right)^2} \tag{78}$$

4. Error Contribution by the Prime Anisoelasticity (4th Harmonic)

From Table 2 and Eq. (75)

$$\sigma_{\Delta\Gamma} = \sqrt{2\Delta f\, N_4(C^2_{xg} + C^2_{yg})(K^2_7 + K^2_8)} \tag{79}$$

5. Error Contribution by the Cross Anisoelasticity

From Table 2 and Eq. (75)

$$\sigma_{\Delta\Gamma} = \sqrt{2\Delta f\left[(N_1 + N_3)C_{zg}^2 + \frac{1}{2}(N_1 + N_3)(C_{xg}^2 + C_{yg}^2)\right]\left(\frac{K_9}{2}\right)^2 + \left(\frac{K_{10}}{2}\right)^2} \tag{80}$$

6. Gradient Error due to Prime Anisoelasticity - Low Frequency Component

$$\sigma = 2\sqrt{\frac{\alpha N_{(0)}}{2}(K_7^2 + K_8^2)} \tag{81}$$

For the RGG $\alpha = 0.1$ and $N_{(0)}$ is the power spectral density at zero frequency.

The errors stated by Eqs. (77), (78), (79), (80) and (81) are at the RGG level.

Table 3 summarizes these equations, and the values quoted are the tensor element values.

E. ERRORS DUE TO MISALIGNMENTS

The RGG sensitivity to misalignments in the earth gravity gradient field at tensor level are:

4.5 EV	Per milliradian tilt off vertical (background gradient assumption)
0.3 EV	Per milliradian misalignment in heading (assumed horizontal principal gradient difference)

Table 3. Error Contribution by the g-Sensitive Terms Expressed in Tensor Element Values

Source	Assumed Power Spectral Density g^2/Hz	Assumed Sensitivity	$\tau_{\Delta\Gamma}$ Error - EUs	
			Uncompensated Hardmounted	Compensated Vibrational Isolator
Differential Arm Mass Unbalance $\tau_{\Delta\Gamma} = \frac{1}{2}\sqrt{\frac{\Delta f}{2}(N_1 + N_3)(K_1^2 + K_2^2)}$ $\Delta f = 0.05$ Hz	$N_1 = 10^{-6}$ $N_3 = 10^{-6}$	$K_1 = 6 \times 10^3$ $K_2 = 6 \times 10^3$	0.95	0.173
Axial Vibrational Torsional Sensitivity $\tau_{\Delta} = \frac{1}{2}\sqrt{\frac{\Delta f}{2} N_2 K_3^2}$ $\Delta f = 0.05$ Hz	$N_2 = 10^{-6}$	$K_3 = 10^4$	0.8	0.145
Prime Anisoelasticity Due to 4th Harmonic $\tau_{\Delta\Gamma} = \frac{1}{2}\sqrt{2\Delta f N_4 (C_{xg}^2 + C_{yg}^2)(K_7^2 + K_8^2)}$ $\Delta f = 0.05$ Hz $C_{xg} = 1$ $C_{xg} = 0$	$N_4 = 10^{-6}$	$K_7 = 500$ $K_8 = 0$	0.08	0.0175
Prime Anisoelasticity Due to Low Frequency $\sigma = \sqrt{\frac{\alpha N_{(0)}}{2}}\sqrt{K_7^2 + K_8^2}$ $\alpha = 0.1$	$N_{(0)} = 10^{-3}$	$K_7 = 500$ $K_8 = 0$	3.5	0.175
Cross Anisoelasticity Due to 1st and 3rd Harmonic $\tau_{\Delta\Gamma} = \frac{1}{2}\sqrt{\frac{\Delta f(N_1 + N_3)}{2}\left(C_{zg}^2 + \frac{C_{xg}^2 + C_{yg}^2}{2}\right)(K_9^2 + K_{10}^2)}$ $\Delta f = 0.05$ Hz $C_{xg} = 0$ $C_{xy} = 0$ $C_{zg} = 1$	$N_1 = 10^{-6}$ $N_3 = 10^{-6}$	$K_9 = 2 \times 10^3$ $K_{10} = 2 \times 10^3$	0.30	0.060

T2151

F. RGG ANGULAR VIBRATIONS ERROR MEASURE FOR ESTABLISHING PLATFORM REQUIREMENTS

$$\sigma_{\Gamma} = \frac{10^9}{4} \sqrt{\int_{-\infty}^{+\infty} S_{\omega}^2(f_s)\, df_s} \tag{82}$$

where

σ_{Γ} error in EV (tensor element value)

$S_{\omega(f_s)}$ power spectral density in $(\text{rad/sec})^2/\text{Hz}$

f_s frequency

SECTION 5

REVIEW OF DATA AND ANALYSIS OF AIRBORNE ENVIRONMENT

Three sources of data were studied and analyzed. These sources were

1. Vibration flight test (Phase I), prepared for the Air Force Weapons Laboratory Kirtland Air Force Base by General Dynamics under contract F29601-71-C-0064, 15 Sept. 71.

2. Prototype moving base gravity gradiometer, Hughes Research Laboratories, R and D Evaluation Report Contract F19628-72-C-022 January 1973.

3. Vibration data for the KC-135 aircraft, memo from Paul H. Merritt to Lt. Col. Jack A. Cook dated 17 May 1976.

The data presented in sources 1 and 3 were measured at cargo tie points in KC-135 aircraft. The measurements were performed without the equivalent mass/inertia of an RGG system in place. Test conditions under which the test data presented by source 2 was obtained were not established. The levels of power spectral densities of linear vibrations obtained from the three sources are presented in Table 4.

Table 4. Power Spectral Density for Linear Vibrations Expressed in G^2/Hz (G in rms values)

Frequency	0	ω_s	$2\omega_s$	$3\omega_s$	$4\omega_s$
Source No. 1	10^{-1}	10^{-6}	10^{-6}	10^{-6}	10^{-6}
Source No. 2	10^{-3}	10^{-6}	10^{-6}	10^{-6}	10^{-6}
Source No. 3	2.5×10^{-3}	16×10^{-6}	17×10^{-6}	17×10^{-6}	17×10^{-6}

It is interesting to note that the test data presented in Source 1 was obtained under moderately harsh environments while the data obtained from source 3 was taken under most benign flight environments. The three sources also contain information pertaining to the angular environments. Graphs in Figures 3 and 4 show the results of these measurements. Data from Source 3 is not included in these figures because it may not be accurate.

It is our opinion that the environmental data presented represents worst case conditions because the measurements were performed without the actual load/inertia of the RGG system.

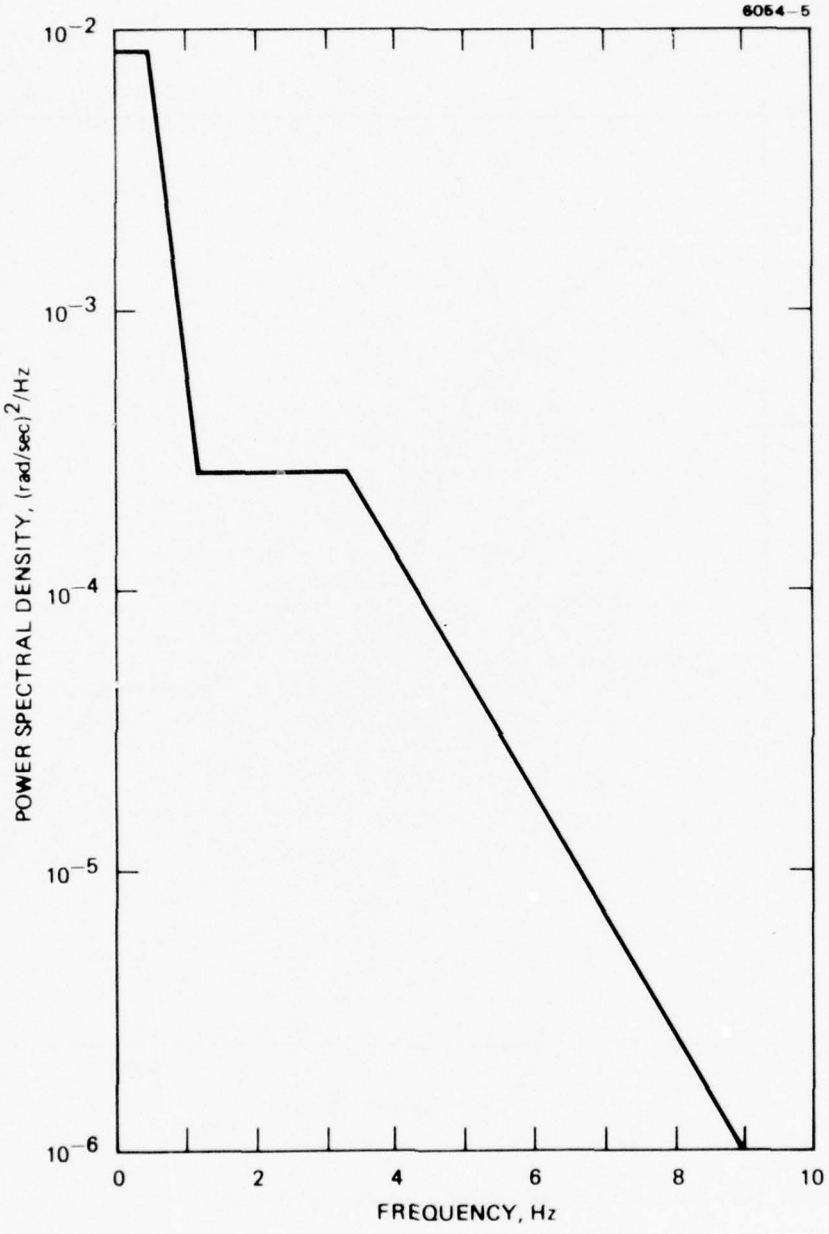

Figure 3. Angular rate power spectrum (reference source No. 1).

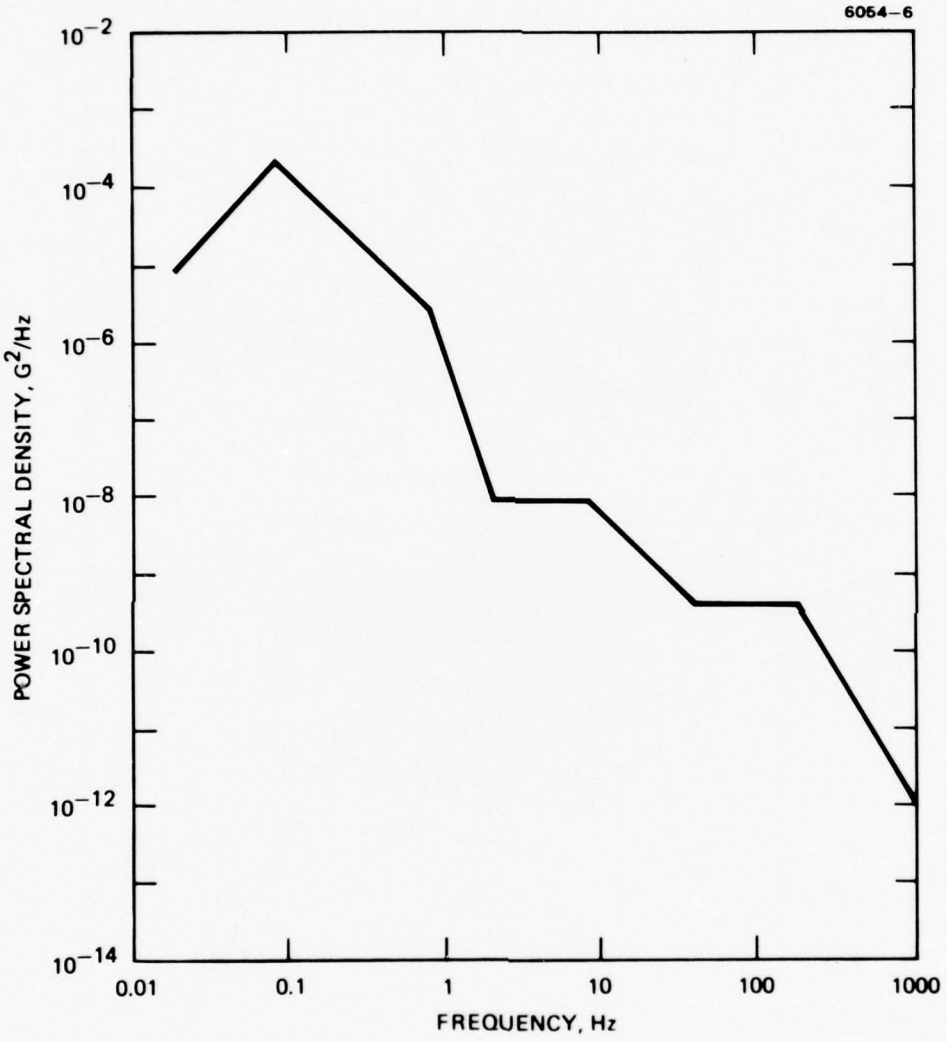

Figure 4. Angular rate power spectrum (reference source No. 2).

SECTION 6

STUDY OF COMPENSATION TECHNIQUES

In this study we assume that the basic RGG sensitivities (the K factors) have been reduced to their goal levels, and thus the resulting error will be a function of the operational environment, the characteristics of the vibration isolation system, and the effectiveness of compensation techniques used.

The vibration isolation system parameters will be selected so that the spin harmonic errors will be reduced to acceptable levels without compensation. Since a practical VIALS cannot limit the rotation field errors and g^2 errors to acceptable levels in the operational environment, these effects will be compensated for.

Compensation for the g^2 errors is relatively straightforward, as conventional accelerometers can be used to measure the acceleration levels. The computational aspects of this compensation are also simple and are shown in Figure 5. Most of the work done in this section deals with compensation for rotational field effects.

Compensation for the rotational fields requires the knowledge of angular velocities at all frequencies. This requirement is difficult to satisfy by using conventional angular rate sensors, and therefore a new sensor is proposed to meet these requirements. The angular velocimeter, as described in this section, can measure angular velocities at all frequencies, and the effectiveness of compensation for the rotational fields can be as high as 1:80.

A. COMPENSATION OF THE RGG OUTPUT FOR THE ROTATIONAL FIELD EFFECTS

Any second-order gradient sensor responds to both gravitational and inertial force gradients. When the sensor is used to measure gravitational force gradients care must be exercised to limit and/or

compensate for any inertial force gradients; presence of such gradients would appear as errors in the measurement of the desired quantity. The output of the RGG sensor is proportional to the source of the angular rate normal to its spin axis, and the effects of the angular rates are minimized by the combined use of the stable platform, shock and vibration isolation system, and compensation. A method of compensation is described in the paragraphs that follow.

1. Rotational Field Compensation Process

The RGG output due to the rotational field effect is

$$\Gamma_{c\omega} = \omega_x^2 - \omega_y^2 \tag{83}$$

$$\Gamma_{s\omega} = -2\omega_x\omega_y \tag{84}$$

The subscripts c and s denote the cosine and sine output channels of the gradiometer, and ω_x and ω_y are the angular input rates resolved along the case-fixed RGG axes. To simplify the description of the compensation process we shall assume that $\omega_y = 0$, $\omega_x = 0$ and then

$$\Gamma_{c\omega} = \omega^2 \tag{85}$$

$$\Gamma_{s\omega} = 0 \tag{86}$$

The block diagram depicting the principle involved in the compensation process for the rotational fields is shown in Figure 5. Using this block diagram we can write for the compensated output of the RGG

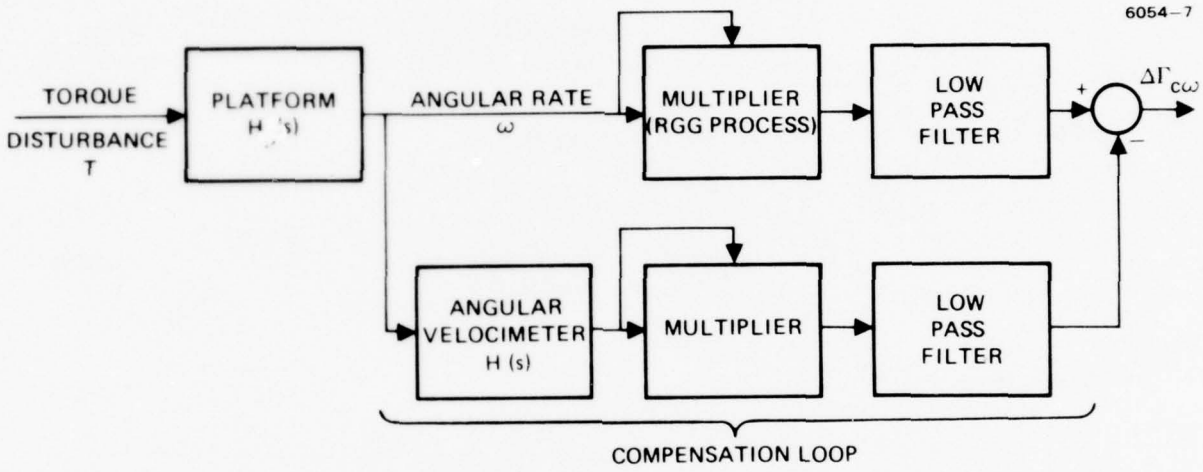

Figure 5. Block diagram of the compensation process for the rotation fields.

$$\Delta\Gamma_{c\omega} = \omega^2 - \omega^2$$

$$= \omega^2 - \left|H_{(s)}\omega\right|^2$$

$$= \omega^2\left(1 - \left|H_{(s)}\right|^2\right) \tag{87}$$

The transfer function of the velocimeter is

$$H_{(s)} = \frac{s^2}{s^2 + 2\zeta\beta_0 s + \beta_0^2} \tag{88}$$

Substitute s = j

$$\left|H_{(s)}\right|^2 = \frac{\left(\frac{\omega}{\beta_0}\right)^2}{\left[1 - \left(\frac{\omega}{\beta_0}\right)^2\right]^2 + 4\zeta\left(\frac{\omega}{\beta_0}\right)^2} \tag{89}$$

Substitute (7) into (5)

$$\Delta\Gamma_{c\omega} = \omega^2 \frac{1 - 2\left(\frac{\omega}{\beta_0}\right)^2 (1 - 2\zeta^2)}{1 + \left(\frac{\omega}{\beta_0}\right)^2 - 2\left(\frac{\omega}{\beta_0}\right)^2 + 4\zeta\left(\frac{\omega}{\beta_0}\right)^2} \tag{90}$$

Assuming that we design a velocimeter with a damping ratio $\zeta = \sqrt{2}/2$ then Eq. (90) reduces to

$$\Delta\Gamma_{c\omega} = \omega^2 \left(\frac{\beta_0^4}{\beta_0^4 + \omega^4} \right) \tag{91}$$

Let

$$\left| H_{eq(s)} \right|^2 = 1 - \left| H_{(s)} \right|^2 \tag{92}$$

Assuming that

$$\Delta\Gamma_{c\omega} = \left| \omega H_{eq(s)} \right|^2 \tag{93}$$

Then comparing Eq. (93) with Eq. (91) we obtain

$$\left| H_{eq(s)} \right|^2 = \frac{\beta_0^4}{\beta_0^4 + \omega^4} \tag{94}$$

Also note that

$$H_{eq(s)} = \frac{\beta_0^2}{s^2 + \sqrt{2}\beta_0 s + \beta_0^2} \tag{95}$$

Validity of Eq. (13) is proven as follows

$$\left|H_{eq(s)}\right|^2 = \left| \frac{\beta_0}{(-j\omega)^2 + \sqrt{2}\ \beta_0(j\omega) + \beta_0^2} \right|^2$$

$$= \left[\frac{\beta_0}{\sqrt{(-\omega^2 + \beta_0^2)^2 + 2\beta_0^2\omega_0^2}} \right]^2$$

$$= \frac{\beta_0^2}{\beta_0^4 + \omega_0^4} \qquad (96)$$

Equation (96) indicates an equivalent process to the compensation described by block diagram of Figure 6 and figure shows the equivalent compensation process for the rotational fields.

2. The Angular Velocity of the Instrument Cluster Caused by the Torque Disturbances

In order that the effects of torque disturbances occurring at all frequencies shall be included we integrate the overall transfer function as indicated by Eq. (97). It is to be noted that Eq. (97) is based on the block diagram for the equivalent compensation process.

$$\Delta\Gamma_{c\omega} = \frac{1}{2\pi} \int_{-\infty}^{+\infty} \left| T\ H_{p(s)}\ H_{eq(s)} \right|^2 d\omega \qquad (97)$$

Assuming that the torque disturbance function, T, is characterized by a constant power spectral density then Eq. (97) becomes

$$\Delta\Gamma_{c\omega} = T^2 I_{eq} \qquad (98)$$

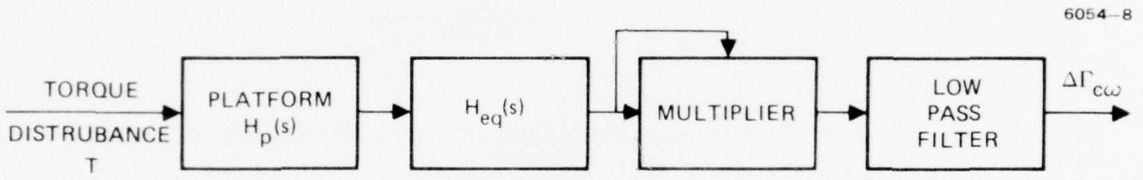

Figure 6. Block diagram of the equivalent compensation process for the rotational fields.

where

$$I_{eq} = \frac{1}{2\pi} \int_{-\infty}^{+\infty} \left| H_{p(s)} H_{eq(s)} \right|^2 d\omega \qquad (99)$$

$H_{p(s)}$ is the platform transfer function relating angular velocity and torque disturbance. This function may have the following form

$$H_{p(s)} = \frac{s}{(s + \alpha_0)(s + \omega_b)} \qquad (100)$$

The uncompensated RGG output in response to the disturbance torques applied to the platform is

$$\Delta\Gamma_{c\omega} = \frac{1}{2\pi} \int_{-\infty}^{+\infty} \left| T H_{p(s)} \right|^2 d\omega \qquad (101)$$

or

$$\Delta\Gamma_{c\omega(u)} = T^2 I_p \qquad (102)$$

where

$$I_p = \frac{1}{2\pi} \int_{-\infty}^{+\infty} \left| H_{p(s)} \right|^2 d\omega \qquad (103)$$

In order that we may estimate the effectiveness of the compensation process discussed here we shall form a ratio between the compensated and uncompensated gradiometer outputs as follows:

$$\frac{\Delta\Gamma_{c\omega}}{\Delta\Gamma_{c\omega(u)}} = \frac{I_{eq}}{I_p} \tag{104}$$

Substituting from Eqs. (99) and (103) we obtain

$$\frac{\Delta\Gamma_{c\omega}}{\Delta\Gamma_{c\omega(u)}} = \frac{1 + \dfrac{\sqrt{2}\ \beta_0}{\alpha_0 + \omega_b}}{2 + \dfrac{\alpha_0\omega_b}{\beta_0^2} + \sqrt{2}\,\dfrac{\alpha_0 + \omega_b}{\beta_0} + \sqrt{2}\ \dfrac{\alpha_0^2\omega_b^2}{\beta_0^3(\alpha_0 + \omega_b)}} \tag{105}$$

Assuming

$$\alpha_0 = 20 \text{ rad/sec} \approx 3.2 \text{ Hz}$$

$$\omega_b = 100 \text{ rad/sec} \approx 16 \text{ Hz}$$

$$\beta_0 = 10 \text{ rad/sec} \approx 1.6 \text{ Hz}$$

The ratio from Eq. (105) becomes

$$\frac{\Delta\Gamma_{c\omega}}{\Delta\Gamma_{c\omega(u)}} \cong \frac{1}{80}$$

This means that for the selected platform and velocimeter parameters the compensation process reduces the error due to rotational field effects by a factor of 80.

B. DESCRIPTION OF THE INCOFLEX ANGULAR VELOCIMETER

The cross-sectional view of the angular velocimeter is shown in Figure 7. The angular velocimeter incorporates three major subassemblies:

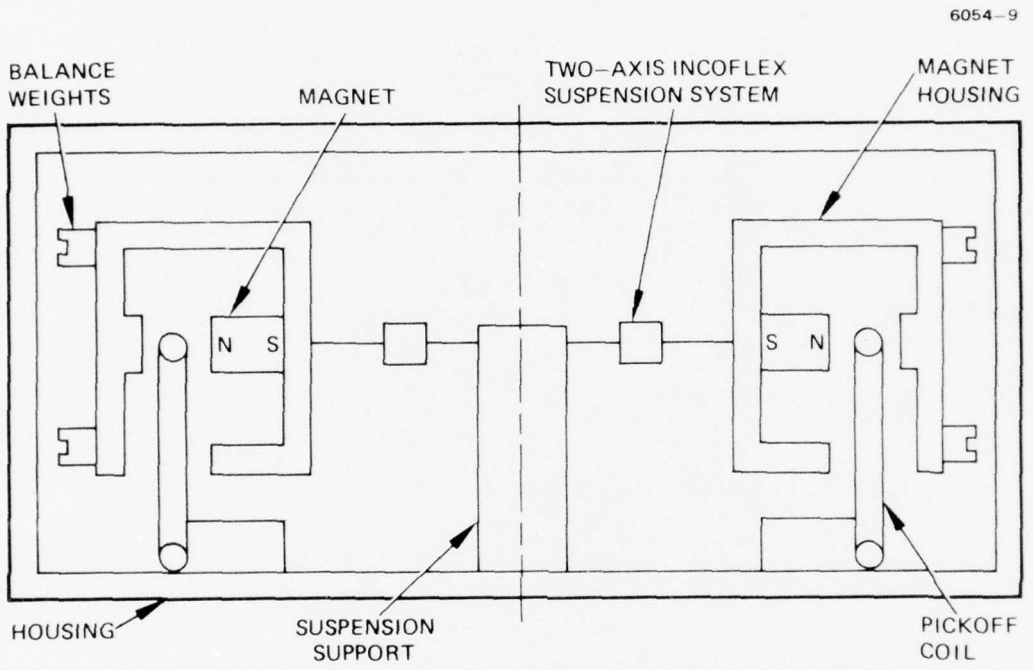

Figure 7. Cross section of the two axis incoflex angular velocimeter.

- Magnet housing
- Two axis suspension system
- Housing

The magnet housing carries a ring magnet which establishes a radially-oriented magnetic field across the airgap. The body of the magnet housing also provides the return path for the magnetic flux. The magnet housing is supported by a two-axis Incoflex suspension system (this is a suspension of a dynamically tuned gyro) which in turn is attached to its support.

Attached to the housing of the velocimeter are four pickoff coils whose upper conductors lie in the magnetic field established by the magnet.

When the housing of the velocimeter is subjected to an angular input rate the attitude of the magnet housing tends to remain fixed and a voltage induced in the pickoff coils is proportional to the relative velocity between the velocimeter housing and the magnet housing. Balance weights attached to the magnet housing are used to eliminate the sensitivity of the velocimeter to translational acceleration inputs.

1. Derivation of the Transfer Function for the Angular Velocimeter

The magnet housing is mechanically coupled to the base of the instrument with a torsional spring rate and damping. The angular motion of the magnet housing related to the angular motion of the base is related by equation (106)

$$(\theta_B - \theta_H)K + (\dot{\theta}_B - \dot{\theta}_H)D = J\ddot{\theta}_H \qquad (106)$$

where

θ_B angle of the velocimeter base

θ_H angle of the magnet housing

K spring constant for the suspension system

D damping coefficient

J combined moment of inertia of the magnet housing and the suspension system about the input axis

Taking Laplace transform of Equation (106) and rearranging

$$\theta_{H(s)} = \frac{D(s) + K}{Js^2 + Ds + K} \theta_{B(s)} \tag{107}$$

But we are interested in the relative angle between the velocimeter base and the magnet housing and therefore

$$\dot{\theta}_{B(s)} - \dot{\theta}_{H(s)} = \dot{\theta}_{B(s)} \frac{Js^2}{Js^2 + Ds + K} \tag{108}$$

The open circuit voltage induced in the pickoff coil is

$$E_{(s)} = K_v(\dot{\theta}_{B(s)} - \dot{\theta}_{u(s)}) \tag{109}$$

Combining Eqs. (108) and (109) we obtain

$$E_{(s)} = \frac{\dot{\theta}_{B(s)}}{K_v} \frac{s^2}{s^2 + 2\zeta\beta_0 s + \beta_0^2} \tag{110}$$

where

K_v voltage constant of the velocimeter

$\zeta = \frac{D}{2\beta_0 J}$ damping coefficient

$B_0 = \sqrt{\frac{K}{J}}$ undamped natural frequency

C. ANGULAR VELOCIMETER EXPERIMENT

1. Purpose

Verify feasibility of the technique and correlate results with calculated data.

2. Description of Test

Standard Incoflex gyro was used in this test. One torquer coil was used to drive the rotor and the diametrically opposite torquer coil was used to indicate the angular velocity of the rotor. The circuit used is shown in Figure 8.

Frequency-Hz	1	3	6	7	8	9	10	11	12	13	20	30	40
E_1 volts P-P	6.2	6.2	3.1	1.75	1.2	0.25	1.25	3.0	3.7	9.0	11.0	12.0	12.0
E_2 mV P-P	1.5	4.5	6.5	6.0	9.5	10.5	9.5	14.5	10.5	13.5	11.5	7.5	5.0

3. Analysis of Test Results

a. Torques Acting on the Rotor

$$T_{(s)} = (Js^2 + Ds + K)\,\theta_{(s)}$$

$$= J\left(s^2 + \frac{D}{J}\,s + \omega_n^2\right)\theta_{(s)}$$

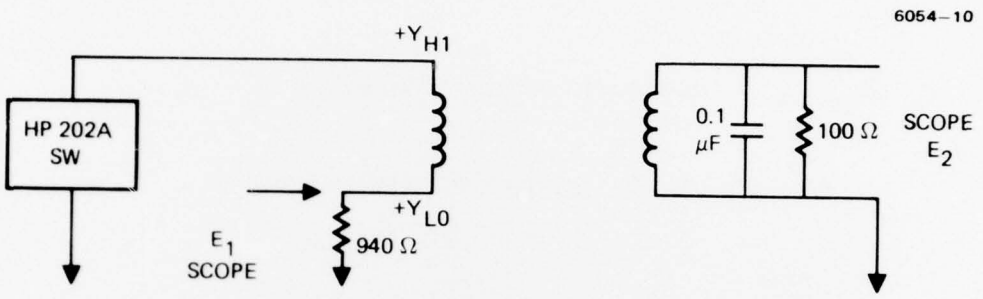

Figure 8. Test set-up.

or

$$\theta_{(s)} = \frac{T_{(s)}}{J\left(s^2 + \frac{D}{J}\, s + \omega_n^2\right)} \tag{111}$$

where $\omega_n^2 = \frac{K}{J}$ (112)

Also

$$\theta_{(s)} = \frac{sT_{(s)}}{J\left(s^2 + \frac{D}{J}\, s + \omega_n^2\right)} \tag{113}$$

For $s \ll \omega_n$ and small damping

$$\dot{\theta}_{(s)} = \frac{sT_{(s)}}{J\omega_n^2} = \frac{sT_{(s)}}{K} \tag{114}$$

For $s \gg \omega_n$ and small damping

$$\dot{\theta}_{(s)} = \frac{sT_{(s)}}{Js^2} = \frac{T_{(s)}}{Js} \tag{115}$$

b. Evaluation of Constants

Gyro torquer scale factor = $2.6^{o}/Hr/\mu a$

Gyro angular momentum = 20,000 gm x cm^2/sec

$$T = \omega H = \frac{1^{o}/hr}{2.06 \times 10^{5}} \times 20,000$$

$$\equiv 0.1 \text{ dyne x cm per } 1^{o}/hr$$

Thus 1 μA produces 0.26 dynexcm when two coils are used in series. For a single torquer coil we have

$K_T = 0.13 \times 10^{6}$ dyne x cm/amp

$J = 15$ gram x cm^2

$K = 50,000$ dyne x cm/radian per axis

$$\omega_n = \left(\frac{50,000}{15}\right)^{1/2} = 57.7$$

$$fn = \frac{1}{2\pi} 57.7 = 9.2 \text{ Hz}$$

Obtain angular velocity of rotor at low frequency - 1 Hz

Torque exerted on rotor = $0.13 \times 10^{6} \times \frac{6.2}{2} \times \frac{1}{940}$

= 428.7 dyne x cm (zero to peak)

Using Eq. (4) angular velocity of rotor

$$\dot{\theta} = \frac{(2\pi \times 1) \times 428.7}{50,000} = 0.054 \text{ rad/sec (zero to peak)}$$

c. Voltage Output

$$E_2 = \frac{1.5 \times 10^{-3}}{2} \text{ volts (zero to peak)}$$

$$K_v = \frac{E_2}{\dot{\theta}} = \frac{1.5 \times 10^{-3}}{2 \times 0.054} = 0.014 \text{ volts/rad/sec}$$

Obtain angular velocity of rotor at higher frequency - 40 Hz

Torque exerted on rotor = $0.13 \times 10^{6} \times \frac{12}{2} \times \frac{1}{940}$

= 830 dyne x cm.

Using Eq. (5) angular velocity of rotor is

$$\dot{\theta} = \frac{830}{15 \times 2\pi \times 40} = 0.22 \text{ rad/sec (zero to peak)}$$

d. Voltage Output

$$E_2 = \frac{5 \times 10^{-3}}{2} \text{ volts 2-P}$$

$$K_v = \frac{E_2}{\dot{\theta}} = \frac{2.5 \times 10^{-3}}{0.22} = 0.011 \text{ volts/rad/sec}$$

e. Calculated Voltage Scale Factor

Calculated voltage scale factor was 0.015 volts/rad/sec (one coil).

In subsequent calculations use

$$K_v = 0.015 \text{ volts/rad/sec per coil}$$

$$K_T = 0.13 \times 10^6 \text{ dyne x cm/amp per coil}$$

4. Summary

Measured value of the voltage constant per coil agrees reasonably well with the computed voltage constant. For further work use

0.015 volts/radian/sec

D. COMPENSATION OF THE RGG OUTPUT FOR ANISOELASTIC EFFECTS

Residual anisoelastic effects (at low frequencies) may be compensated for from the knowledge of accelerations and the residual sensitivities K_7 and K_8 for the RGG instrument. Three accelerometers will be used to measure the components of acceleration and the data will be processed in the computer in accordance with the block diagram

shown in Figure 9. We expect that compensation will reduce this by a factor of 20.

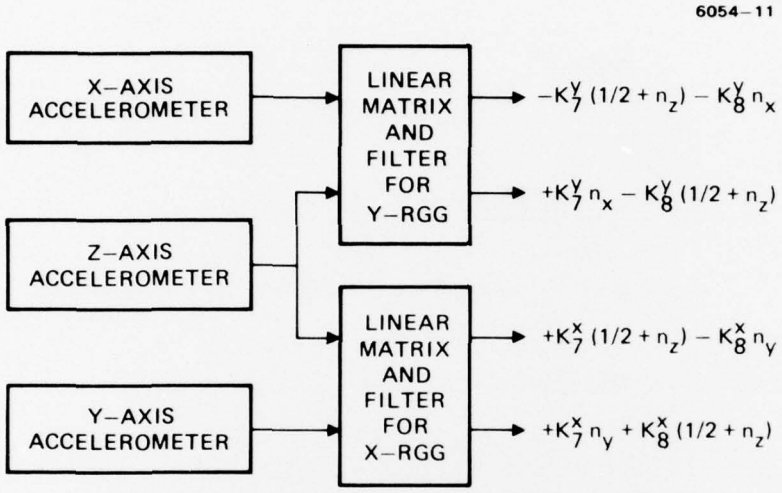

Figure 9. Compensation of the RGG (SAW) for aniso-elastic effects.

SECTION 7

VIALS SPECIFICATION

A. DESCRIPTION

The three RGG sensors shall be mounted to the stable element of a three-axis platform. The platform in turn shall be supported by a C.G.* vibration isolation mount for isolation of translational and rotational vibrations. The three-axis platform provides long-term azimuth and level stabilization of the RGG cluster. In addition to the RGG cluster the stable element may carry gyros and accelerometers required for stabilization purposes, and also angular velocimeters and translational accelerometers required for compensation purposes.

B. VIALS REQUIREMENTS FOR AIRBORNE MAPPING MISSION

The VIALS system design shall assure proper operation of the RGG cluster in an airborne environment (benign class) typified by a KC-135 aircraft. The required accuracy of the RGG sensors, expressed as tensor elements, shall be within 1.0 EU (one sigma) during a 10-hour flight.

C. ENVIRONMENT - OPERATING

Data shall be taken when the aircraft is flown in straight and level cruise condition during non-turbulent weather. The cruise conditions shall be as follows:

---

*Prevents conversion of translational inputs into rotation of the stable element.

Altitude	25,000 to 30,000 ft
Ground Speed	400 to 500 mph
Cabin Temperature:	72 ± 3 F
Cabin Pressure:	Between sea level and 10,000 ft equivalent pressure altitude will be maintained at all times.

The aircraft motion environment shown in Figures 10 and 11 shall be applicable and shall apply to all axes.

D. FUNCTIONAL AND PERFORMANCE REQUIREMENT

1. Vibration Isolation Mount

The vibration isolation mount shall support the weight of the platform and stable element containing the RGG sensors, stabilization gyros, and accelerometers, compensation instruments, and electronics associated with the above equipment. The mount shall provide three translational degrees-of-freedom.

a. Load Capacity

The vibration isolation mount shall provide the specified vibration attenuation while supporting its payload and while being exposed to vibration spectra specified in Section 3 and when exposed to aircraft maneuver loads of 0.1 G.

b. Elastic Center

The distance between the center of mass of the payload and the effective elastic center of the vibration isolation mount shall not exceed 0.2 inches.

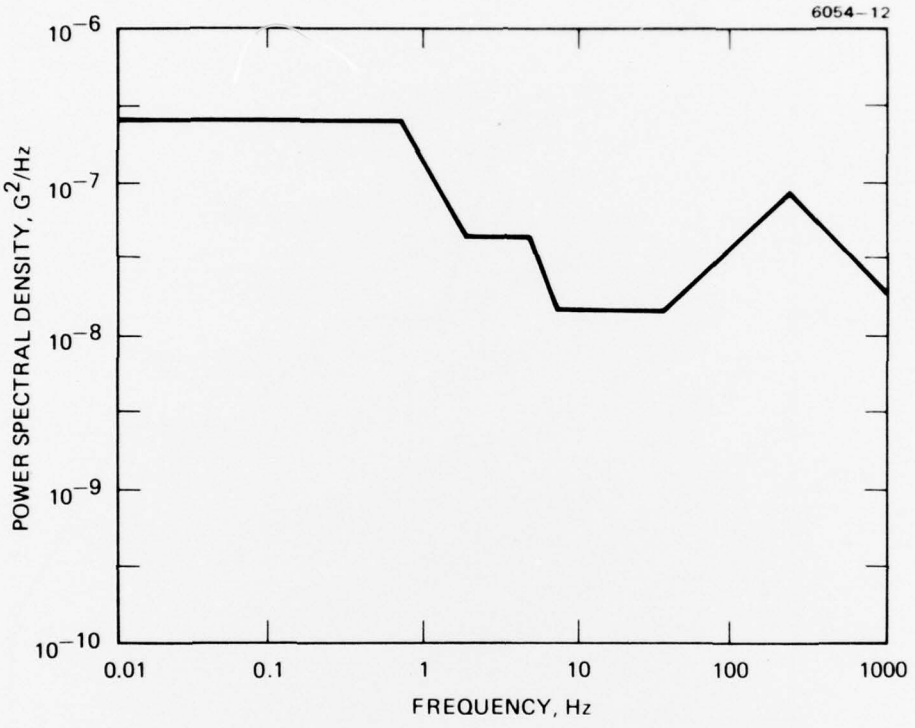

Figure 10. Acceleration power spectra.

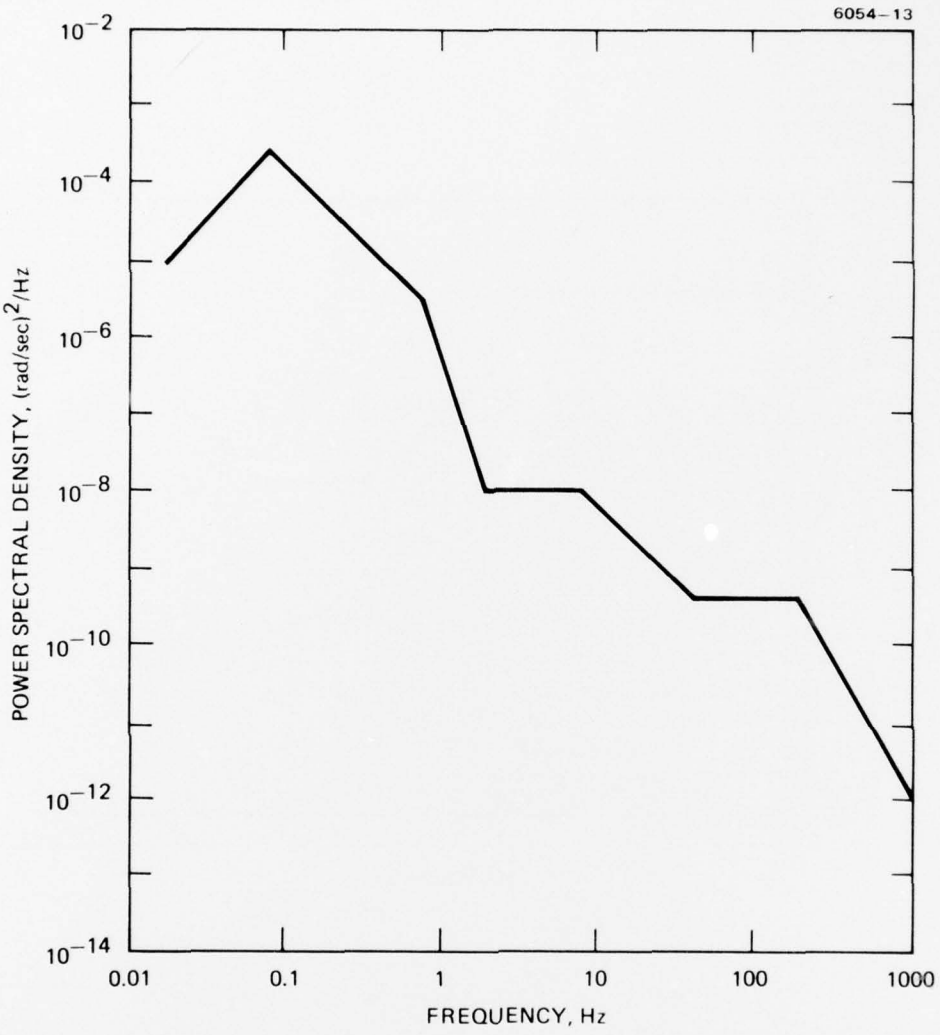

Figure 11. Angular rate power spectrum.

c. Mass Balance

The vibration isolation mount shall be equipped to provide for mass balancing of its load so that the distance as defined in 7.D.1.b (above) can be adjusted to be within 0.1 inches.

d. Translational Vibration Attenuation

The vibration isolation mount shall provide for isolation of translational vibration in all three axes. The translational isolation performance in any axis shall equal or exceed the performance characterized by a second-order linear system having natural frequency 2 Hz ± 0.5 Hz and maximum amplification not exceeding 1.2.

2. Stable Platform

The stable platform shall meet the following performance requirements while supporting its payload and when mounted on the vibration isolation mount whose characteristics are specified in 7.D.1.

a. Reference Stabilization Axes

The stable platform shall provide three-axis stabilization such that locally-level, true-north-referenced, stable element orientation is maintained.

b. Angular Freedom

The stable platform shall be capable of accommodating aircraft motion excursions of ±30 degrees in pitch and roll while in any heading orientation. The platform shall have 360 degrees of freedom in azimuth.

c. Gimbal Readout

Angle transducers providing gimbal angles for each of the three axes will be provided. These transducers shall have an overall accuracy of 1 arcminute.

d. Angular Alignment Accuracy

Initial alignment accuracy and allowable drift limits are as specified below.

1. Platform and RGG Initialization – The accuracies required for initial alignment of the sensor cluster are as follows:

Vertical:	5×10^{-5} radian, 1 sigma with respect to plumb-bob vertical
Azimuth:	5×10^{-4} radian, 1 sigma with respect to north reference

After initial alignment of the sensor cluster, RGG initialization will be accomplished. This RGG initialization process may require up to one hour to complete. The platform drift requirement shall apply during the RGG initialization period. No retrimming or adjustments of the stable platform is allowed at any time during the ensuing 10 hr operational run after RGG initialization has commenced.

2. Allowable Drift – The angular orientation of the stable element shall not drift from the initially aligned reference by more than the following amounts for a flight of 10 hours duration:

Level:	10^{-4} radian
Azimuth:	10^{-3} radian

e. Stable Platform Computer

A stable platform computer whose accuracy is compatible with meeting the alignment accuracy requirements will be required.

f. Payload Description

The weight and size of the three RGG sensors shall be as follows:

Weight	TBD
Size	TBD

(1) Compensation Accelerometers

Number Required	3
Weight	TBD
Size	TBD

(2) Compensation Angular Velocimeters

Number Required	2
Weight	TBD
Size	TBD

(3) Level Accelerometers

Number Required	2
Weight	TBD
Size	TBD

(4) Level and Azimuth Gyros

Number Required	2
Weight	TBD
Size	TBD

g. Power and Signal Transmission

Slip rings or their equivalent will be required to transmit power to and signals from the payload equipment as follows:

ac power	TBD
dc power	TBD
Signals:	
RGGs	32 channels
Gyros	TBD
Accelerometers	TBD
Angular velocimeters	TBD

h. Reaction Torques from Payload

(1) Sensor rotor mass unbalance – each sensor rotor mass unbalance shall not exceed 7.5×10^{-5} lb x in. Each sensor is operated at a nominal spin frequency equal to 1050 RPM.

(2) Sensor angular momentum – the angular momentum of each sensor is 30.1×10^{6} gram x cm^2/sec.

REFERENCES

1. Rotating Gravity Graviometer Research and Development Design and Evaluation Report, Hughes Research Laboratories, March 1976.

2. R. W. Peterson memo, "Orientation Error Sensitivities of a Gradient Measure Systems," 11 December 1973.